In presenting this dissertation as a partial fulfillment of the requirements for an advanced degree from the Georgia Institute of Technology, I agree that the Library of the Institute shall make it available for inspection and circulation in accordance with its regulations governing materials of this type.

I agree that permission to copy from, or to publish from, this dissertation may be granted by the professor under whose direction it was written, or, in his absence, by the Dean of the Graduate Division when such copying or publication is solely for scholarly purposes and does not involve potential financial gain.

It is understood that any copying from, or publication of, this dissertation which involves potential financial gain will not be allowed without written permission.

Raja M. Bitar

EFFECT OF AXIAL THRUST AND DEFLECTIONS ON THE ULTIMATE LOAD OF GABLE FRAMES

A THESIS

Presented to

the Faculty of the Graduate Division

by

Raja M. Bitar

In Partial Fulfillment

of the Requirements for the Degree

Master of Science in Civil Engineering

Georgia Institute of Technology

January, 1958

7a
12R

EFFECT OF AXIAL THRUST AND DEFLECTIONS ON THE ULTIMATE LOAD OF GABLE FRAMES

Approved:

Dr. F. W. Schutz, Jr.

Dr. M. R. Carstens

Prof. James R. Fincher

Date approved by Chairman: Dec 13, 1957

To my parents,

MR. & MRS. MULHIM BITAR

ACKNOWLEDGMENTS

The writer wishes to express his grateful appreciation to Dr. F. W. Schutz for guidance, assistance, and encouragement in the preparation of this dissertation.

Thanks are due to Dr. B. M. Drucker for his friendly and invaluable assistance in the use of the computer. Thanks are also due to Professor J. R. Fincher and Dr. M. R. Carstens, members of the reading committee, whose courteous and constructive criticisms have been so helpful in the final phase of preparation of this dissertation.

To Mr. C. M. Pavey of the Civil Engineering Department machine shop go thanks for the invaluable assistance in fabricating the test equipment.

TABLE OF CONTENTS

LIST OF TABLES

LIST OF FIGURES

LIST OF FIGURES (continued)

LIST OF FIGURES (continued)

LIST OF SYMBOLS

A = area of section

A_1 = axial thrust associated with k_1

A_2 = axial thrust associated with k_2

A_3 = axial thrust associated with k_3

Ay = load at yield

H_L = left horizontal force

H_R = right horizontal force

E = Young's modulus of elasticity

I = moment of inertia about the x-x axis

L = unit length

M = moment

Mp = plastic moment

MF = fixed end moment

P = total load

R_L = left reaction

R_R = right reaction

Z = plastic modulus

b = width of section

d = deflection

dv = vertical deflection

dh = horizontal deflection

f = shape factor

LIST OF SYMBOLS (continued)

k = reduction coefficient due to axial thrust

p = unit load

h = rise

ϵ = unit strain

σ = unit stress

σy = yield stress

γ = unit rotation

Ψ = total rotation

θ = relative rotation

α = angle of elevation

SUMMARY

EFFECT OF AXIAL THRUST AND DEFLECTIONS ON THE ULTIMATE LOAD OF GABLE FRAMES

The objective of this investigation is to determine the effect of both the axial thrust and deflections on the ultimate load carrying capacity of gable frames. The method involves the use of the interaction of axial force and ultimate moment in any given member of a structure, then superimposing the secondary effect of deflection by taking into consideration the new configuration of the structure prior to collapse.

A rational approach has been developed for the analysis, and equations have been derived to compute the ultimate load the structure is capable of carrying. The analysis was developed for a rectangular section, neglecting the effects of shear and stability, with the assumption that the material to be used was A-7 structural steel.

The experimental work to verify the theoretical development included tests on 22 gable frame models having different rise-to-span ratios and different column heights. The deflections and ultimate load of the tested models were recorded and graphs were plotted to show the correlation between the analysis and the test results. In this study, the "ultimate load" is defined as the load at which a mechanism has been formed in the structure and where excessive deformations occur at no increase in load.

Since the models had to be welded, the steel was annealed to relieve any residual stresses and provide a material less likely to be affected by welding. The welds did, however, create a local effect, which did not affect the ultimate load to any appreciable degree.

From the test results it was observed that the reduction in the ultimate load due to both deflections and axial load could be predicted in gable frames and that the general approach is applicable to WF shapes as well as to rectangular sections.

A premature failure of the models occurred at a lower ultimate load than predicted by the simple plastic theory, and the deflections at failure were smaller than the calculated deflections which were associated with the higher theoretical ultimate load.

Theoretical calculations as well as graphs are presented to reveal the correlation between the theoretical analysis, the experimental work, and the solution by the simple plastic theory.

CHAPTER I

INTRODUCTION

The simple concepts of plastic analysis and the usual design techniques ignore the effect of deflections and assume that the structure does not deform excessively. This criteria is satisfied for most structures having horizontal and vertical members.

The effect of axial load on the ultimate load is fully outlined by L. S. Beedle, B. Thurlumann, and R. L. Ketter (1).* The assumptions made are:

(a) Plane sections remain plane
(b) Idealized σ-ϵ relationship (Fig. 1)
(c) Small deflections, i.e., $\tan \phi = \phi$
(d) Equilibrium (from stress distribution)

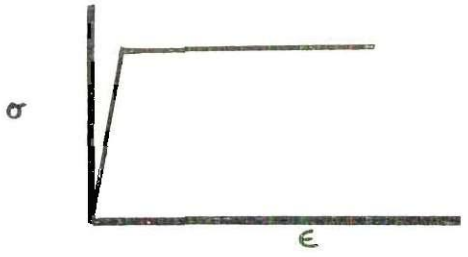

Fig. 1

In this study, interaction equations and graphs are presented to take account of the reduction of "Mp" (the plastic moment) due to "P" (the axial force) on any member of the structure.

---

*Numbers in parenthesis indicate references listed in the "Literature Cited" section of the bibliography.

Stability was ignored in this presentation, for it is assumed that the structure is fully braced against lateral buckling. Lateral buckling does not present a problem in gable frames where a rectangular section is used. It is more important in the case of WF sections. Shear was also ignored since its effect is negligible, for even in those cases where it cannot be taken by the elastic core of the section, the phenomena of strain hardening is adequate to take care of shear.

The objective of this investigation was to determine the following:

1. The effect of the deflections on the ultimate load
2. The effect of the axial force on the ultimate load
3. The behavior of the structure and the mode of failure at collapse
4. The development of a design procedure taking into account the effect of axial force and deflections

The experimental procedure was intended to verify the analytical phase of this investigation. Tests were carried out on gable frame models made of 3/16" square rods having characteristics similar to A-7 steel. The rise-to-span ratios and the height of columns were varied to show the effect of deflections and axial load with the variation of these ratios.

The analytical phase included the calculation of the reduction of "Mp" (the ultimate moment) at each possible hinge location by first taking into account the effect of axial force, then superimposing the reduction in the ultimate load, "P", due to deflections, i.e., the effect of the change of shape of the structure before collapse.

CHAPTER II

THEORETICAL DEVELOPMENT

In the presentation of this analysis, it is assumed that the reader is familiar with the terminology and fundamental concepts of plastic design.

The plastic solution of any frame has to fulfill the following conditions: (1)

1. Equilibrium
2. Plasticity condition ($M \leq Mp$)
3. Mechanism (additional deformations are possible without increase of load (sufficient Mp's))

A lower bound solution is when equilibrium conditions are satisfied and no violation of plasticity exists. Thus, the loads are lower than, or equal to, the true ultimate load since a mechanism may not exist due to the lack of enough hinges.

Where equilibrium conditions are satisfied and a mechanism exists, we have an upper bound solution. The lowest of the upper bounds is the correct solution and will be equal to the highest possible lower bound. A mechanism consists of enough hinges to cause the framework to collapse in a local or general fashion. These hinges can occur:

1. Under a concentrated load
2. At a change of section
3. At a change of direction in the members
4. Where shear is zero

Each hinge removes one degree of indeterminancy in the structure.

Three general shapes of gable frames under the same loading were investigated, as shown below:

Type I

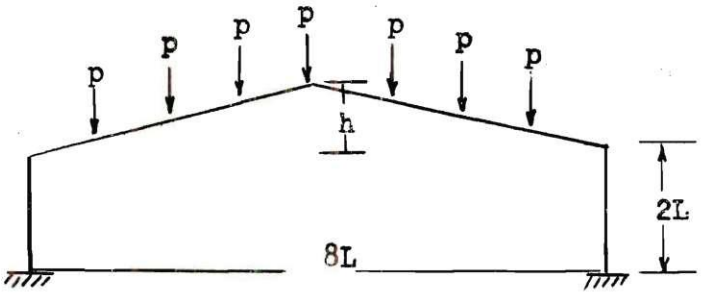

Fig. 2

Type II

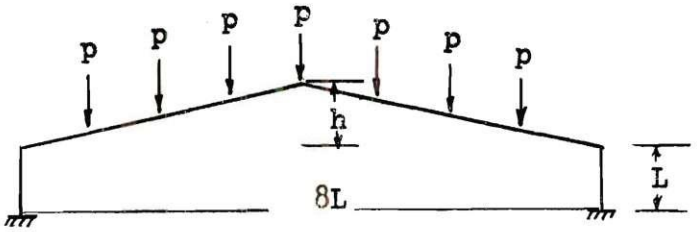

Fig. 3

Type III

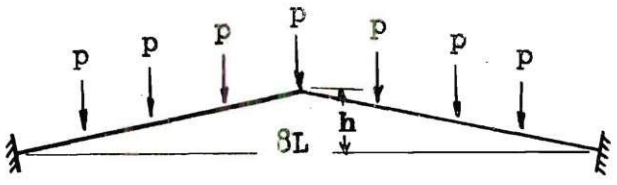

Fig. 4

Reduction in Mp due to influence of axial thrust on plastic moment capacity: -- If a member is subjected to both an axial thrust and a bending moment, the progressive change in stress distribution across a section as these loads are increased will be of the form shown in Fig. 5.

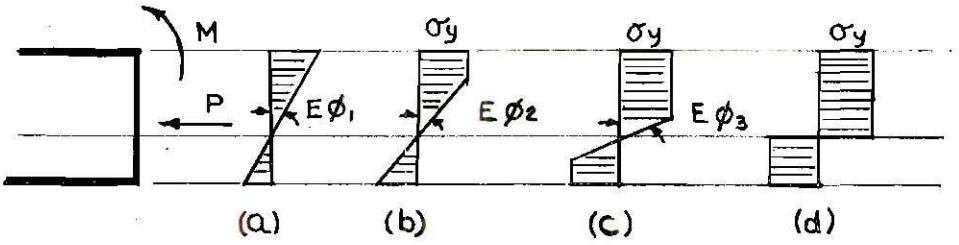

Fig. 5

Since a plastic hinge is based on infinite ϕ value, then Mp k will be determined from consideration of the stress distribution. For a rectangular section, Eq. (1) from Ref. 2 applies:

$$k = \frac{Mpc}{Mp} = 1 - \left(\frac{P}{Py}\right)^2 \tag{1}$$

$$Mp = \sigma y\, Z \tag{2}$$

$$\sigma y = \frac{Mp}{Z} \tag{3}$$

and,

$$Py = \sigma y\, A \tag{4}$$

$$Py = \frac{Mp}{Z}\, A \tag{5}$$

For a square section,

$$A = b^2 \tag{6}$$

$$Z = \frac{b^3}{4} \tag{7}$$

Then,

$$Py = \frac{4Mp}{b} \tag{8}$$

In the development of this analysis, the coefficient "k" allows for the reduction in the ultimate moment at every hinge location due to axial force after the correct collapse mechanism is determined.

Equations have been derived to find the values of "k's" and these values for the different ratios of rise-to-span and column heights are listed in Table 4.

Finding values of "k's" for Types I and II: -- The failure mechanism and method of approach to finding the "k" values for Types I and II are identical. An example below illustrates the procedures:

Loading diagram:

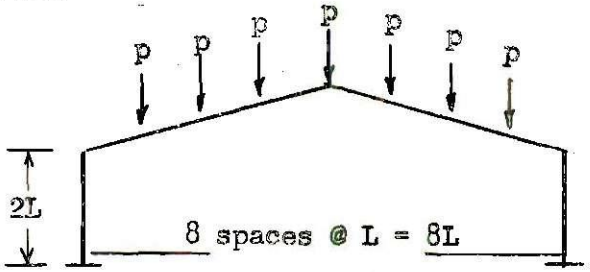

Fig. 6

Moment diagram showing moment peaks:

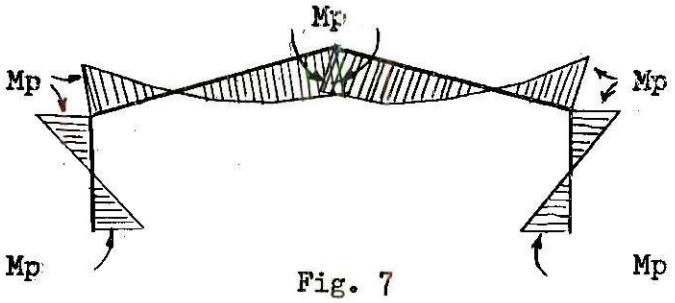

Fig. 7

The correct failure mechanism:

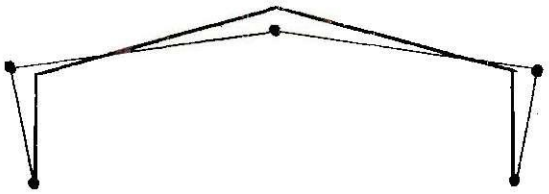

Fig. 8

This mechanism fulfills:

Plasticity
Mechanism
Equilibrium

Since there is symmetry, it is advantageous to use the instantaneous center method on half the structure as shown below:

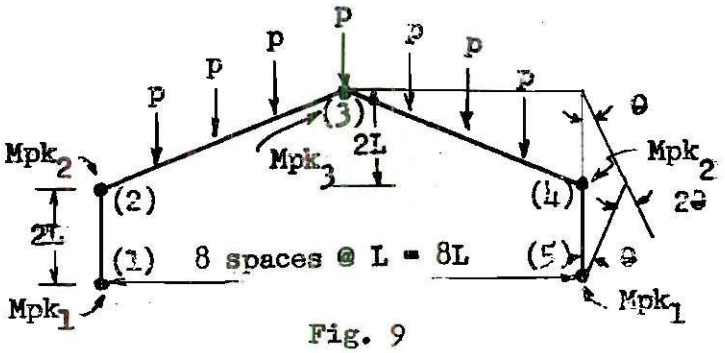

Fig. 9

We now have:

$$Mp\ \theta\ (k_1 + 2k_2 + k_3) = pL\ \theta\ (1 + 2 + 3 + 4/2) \qquad (9)$$

$$p = \frac{Mp}{8L}\ (k_1 + 2k_2 + k_3) \qquad (10)$$

The total ultimate load is: $P = 7p$ (11)

Now the structure is determinate, since enough hinges have been formed to relieve indeterminance. Since our original structure is

indeterminate to the third degree, hinges 1 and 4 and hinges 1 and 5 occur simultaneously due to symmetry of the structure and of the loading condition. Applying statics, we have from Fig. 10:

$$R_L = R_R = \frac{7p}{2} \tag{12}$$

Summing moments about "B" (from Fig. 10):

$$Mpk_2 + Mpk_1 - 2L\,(H_L) = 0$$

$$H_L = H_R = \frac{Mp}{2L}\,(k_1 + k_2) \tag{13}$$

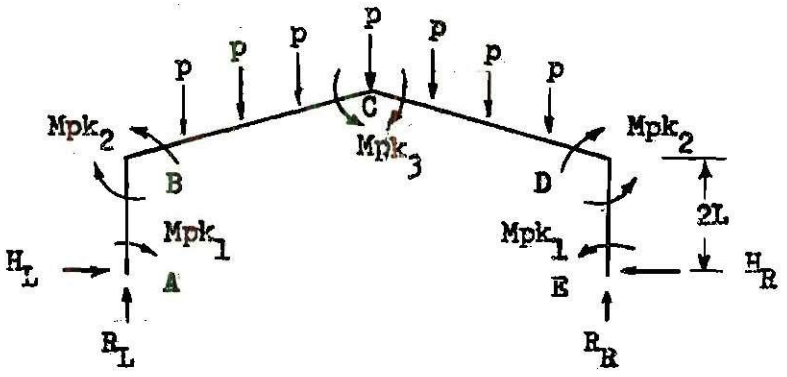

Fig. 10

A_1 is the axial load associated with k_1; A_1 or A_2, whichever is greater, is the axial load associated with k_2; A_3 is the load associated with k_3. It follows that:

$$A_1 = \frac{7p}{2} \tag{14}$$

$$A_2 = H\cos\alpha + R\sin\alpha \tag{15}$$

$$A_3 = H\cos\alpha \tag{16}$$

$$\tan\alpha = \frac{h}{4L} \tag{17}$$

From Eqs. (10) and (14) we have:

$$A_1 = \frac{7Mp}{16L}(k_1 + 2k_2 + k_3) \tag{18}$$

From Eqs. (8) and (18) we get:

$$\frac{A_1}{Ay} = \frac{7b}{64L}(k_1 + 2k_2 + k_3) \tag{19}$$

Values of "b" and "L" are obtained from Tables 1 and 2, then substituted in Eq. (19) as follows:

$$\frac{A_1}{Ay} = 0.01023k_1 + 0.02046k_2 + 0.01023k_3 \tag{20}$$

Using Eq. (1) we get:

$$k_1 = 1 - (0.01023k_1 + 0.02046k_2 + 0.01023k_3)^2 \tag{21}$$

Substituting the values of "H" and "R" in Eq. (15) for A_2 we obtain:

$$A_2 = \frac{Mp}{2L}(k_1 + k_2)\frac{4L}{\sqrt{20L^2}} + \frac{7Mp}{16L}(k_1 + 2k_2 + k_3)\frac{2L}{\sqrt{20L^2}} \tag{22}$$

if $A_2 > A_1$

Where:

$$\frac{4L}{\sqrt{20L^2}} = \cos\alpha \tag{23}$$

$$\frac{2L}{\sqrt{20L^2}} = \sin\alpha \tag{24}$$

Then from Eqs. (8) and (22) we get:

$$\frac{A_2}{Ay} = \frac{b}{2\sqrt{20L^2}} (k_1 + k_2) + \frac{2L}{\sqrt{20L^2}} \left(\frac{7b}{64L}\right) (k_1 + 2k_2 + k_3) \qquad (25)$$

Substituting the values of "b" and "L" from Table 1:

$$\frac{A_2}{Ay} = 0.01505k_1 + 0.02043k_2 + 0.00458k_3 \qquad (26)$$

Substituting Eq. (26) in Eq. (1) we obtain:

$$k_2 = 1 - (0.01505k_1 + 0.02043k_2 + 0.00458k_3)^2 \qquad (27)$$

if $k_2 < k_1$

Substituting the value of "H" from Eq. (13) in Eq. (16), we get:

$$A_3 = \frac{Mp}{2L} (k_1 + k_2) \frac{4L}{\sqrt{20L^2}} \qquad (28)$$

From Eqs. (8) and (28) we obtain:

$$\frac{A_3}{Ay} = \frac{b}{2\sqrt{20L^2}} (k_1 + k_2) \qquad (29)$$

Substituting the values of "b" and "L" from Table 1:

$$\frac{A_3}{Ay} = (0.01047k_1 + 0.01047k_2) \qquad (30)$$

From Eqs. (1) and (30) we obtain:

$$k_3 = 1 - (0.01047k_1 + 0.01047k_2)^2 \qquad (31)$$

These equations can be set in a general form as shown below:

$$k_1 = 1 - (Ak_1 + Bk_2 + Ck_3)^2 \tag{32}$$

$$k_2 = 1 - (Dk_1 + Ek_2 + Fk_3)^2 \text{ if } k_2 < k_1 \tag{33}$$

$$k_2 = k_1 \text{ if } k_2 > k_1 \qquad \text{(for Types I and II)}$$

$$k_3 = 1 - (Gk_1 + Hk_2 + Ik_3)^2 \tag{34}$$

A, B, C, D, E, F, G, H, and I are constants for: (1) a definite loading condition; (2) a ratio of rise-to-span and column height; and (3) a definite shape section.

The values of "k_1", "k_2", and "k_3" were obtained by programming these equations on an IBM 650 electronic computer.

Eqs. (32), (33), and (34) are also applicable to WF sections as long as the neutral axis is in the web. The values of A, B, C, D, E, F, G, H, and I will vary with the values of:

$(\frac{A^2}{4wZ}$ and $\frac{P}{Py})$ where "w" is the thickness of the web

from Beedle (1):

$$\frac{Mpc}{Mp} = 1 - \frac{A^2}{4wZ}\left(\frac{P}{Py}\right)^2 \tag{35}$$

A semi-graphical method of finding the "k" values of WF sections is shown in Appendix C. This method applies to any section that has a known "load-moment" interaction curve.

Finding values of "k's" for Type III: -- Ignoring the effect of deflection on this type of structure, the solution by the simple plastic theory is readily available. The treatment of the analysis is shown below for the case where the rise is "2L":

Loading diagram:

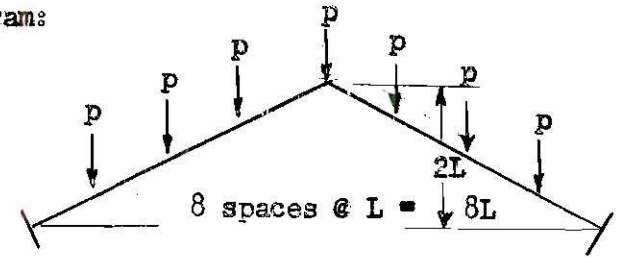

Fig. 11

The moment diagram associated with the loading:

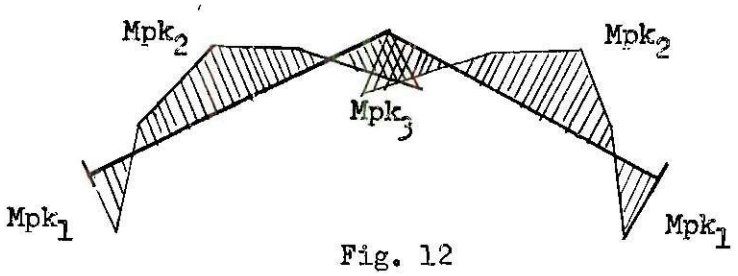

Fig. 12

Correct failure mechanism and taking symmetry into consideration:

Fig. 13

This mechanism fulfills:

Plasticity
Mechanism
Equilibrium

This solution is general and applies to all Type III models, irrespective of the rise. Due to the presence of symmetry, half of the structure is analyzed:

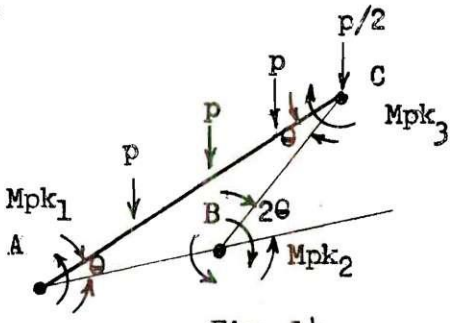

Fig. 14

Thus we obtain:

$$Mp\ \theta\ (k_1 + 2k_2 + k_3) = 2pL\theta\ (1 + 1) \tag{36}$$

$$p = \frac{Mp}{4L}\ (k_1 + 2k_2 + k_3) \tag{37}$$

$$P = 7p \tag{38}$$

Now the structure is determinate and all the forces can be obtained from statics:

Taking member AB as a free body:

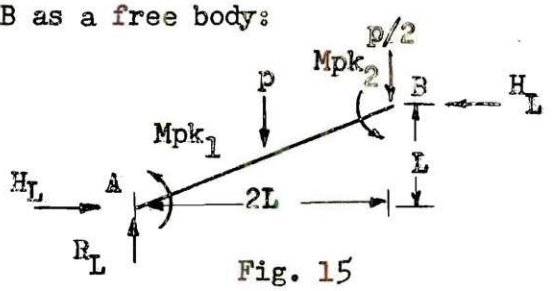

Fig. 15

From symmetry:

$$R_R = \frac{7p}{2} \tag{39}$$

Taking moments about B:

$$- Mp\,(k_1 + k_2) - pL - H_L L + \frac{7p}{2}(2L) = 0 \tag{40}$$

$$H_L = \frac{1}{L}\left[6pL - Mp\,(k_1 + k_2)\right] \tag{41}$$

Taking member BC as a free body:

$$R_{L1} = \frac{5p}{2} \tag{42}$$

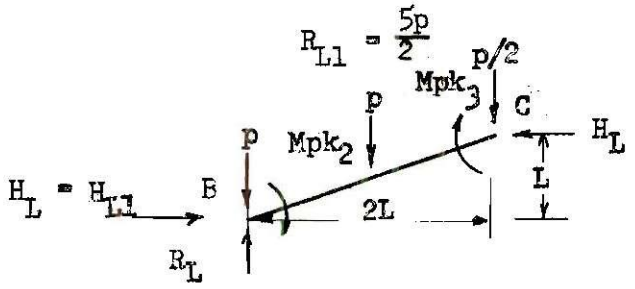

Fig. 16

Taking moments about C:

$$Mp\,(k_2 + k_3) - pL\,(1 + 2) - H_{L1} L + \frac{5p}{2}(2L) = 0 \tag{43}$$

$$H_{L1} = \frac{1}{L}\left[2pL + Mp\,(k_2 + k_3)\right] = H_L \tag{44}$$

It follows that:

$$A_1 = R_L \sin\alpha + H_L \cos\alpha \tag{45}$$

$$A_2 = R_{L1} \sin\alpha + H_{L1} \cos\alpha \tag{46}$$

$$A_3 = H_{L1} \cos\alpha \tag{47}$$

Substituting the values of "p", cos , and sin from Eqs. (37), (23), and (24) in Eq. (44) we obtain:

$$A_1 = \frac{4L}{\sqrt{20L^2}} \cdot \frac{1}{L} \left[\frac{6L(Mp)}{4L} (k_1 + 2k_2 + k_3)\right] - Mp(k_1 + k_2)$$

$$+ \frac{2L}{\sqrt{20L^2}} \left[\frac{7Mp}{8L} (k_1 + 2k_2 + k_3)\right] \qquad (48)$$

Dividing by "Ay", as in Eq. (8):

$$\frac{A_1}{Ay} = \frac{b}{\sqrt{20L^2}} (0.5k_1 + 2k_2 + 1.5k_3) + \frac{7b}{16\sqrt{20L^2}} (k_1 + 2k_2 + k_3) \qquad (49)$$

Now, substituting values of "b" and "L" in Eq. (49), we obtain:

$$\frac{A_1}{Ay} = (0.019675k_1 + 0.061340k_2 + 0.040665k_3) \qquad (50)$$

Using Eq. (1):

$$k_1 = 1 - (0.019675k_1 + 0.061340k_2 + 0.040665k_3)^2 \qquad (51)$$

Now for A_2, substituting values of "p" from Eq. (37) in Eq. (46), we obtain:

$$A_2 = \frac{4L}{\sqrt{20L^2}} \cdot \frac{1}{L} \left[(2L \frac{(Mp)}{4L} (k_1 + 2k_2 + k_3) + Mp(k_2 + k_3)\right]$$

$$+ \frac{2L}{\sqrt{20L^2}} \left[\frac{5p}{8L} (k_1 + 2k_2 + k_3)\right] \qquad (52)$$

Dividing by "Ay":

$$\frac{A_2}{Ay} = \frac{b}{\sqrt{20L^2}} (0.5k_1 + 2k_2 + 1.5k_3) + \frac{5b}{16\sqrt{20L^2}} (k_1 + 2k_2 + k_3) \qquad (53)$$

Substituting values of "b" and "L" from Table 1, we get:

$$\frac{A_2}{Ay} = (0.017045k_1 + 0.055080k_2 + 0.038035k_3) \qquad (54)$$

And from Eq. (1), we have:

$$k_2 = 1 - (0.017045k_1 + 0.055080k_2 + 0.038035k_3)^2 \qquad (55)$$

Similarly, for A_3:

$$\frac{A_3}{Ay} = \frac{b}{\sqrt{20L^2}} (0.5k_1 + 2k_2 + 1.5k_3) \qquad (56)$$

And:

$$k_3 = 1 - (0.010495k_1 + 0.041980k_2 + 0.031485k_3)^2 \qquad (57)$$

Eqs. (51), (55), and (57) are set in the same general form as Eqs. (33), (34), and (35). Table 4 gives the values of A, B, C, D, E, F, G, H, and I for the different cases.

Computation of deflection: -- In the computation of deflections, the slope deflection equations were used. The method is outlined by Neal (2). The assumptions and conditions are:

(a) Idealized M - Ø relationship
(b) Each span retains its flexual rigidity for the whole length between hinges
(c) Unlimited rotation is possible at hinge sections M = Mp

Contrary to their use in elastic design, where the slope deflection equations are used to determine the moments at the various sections, in plastic design the moments are all known and the slope

deflection equations are used to determine relative deflection of segments of the structure.

To obtain the deflection of a structure at ultimate load, the following information is needed:

(a) Moment diagram at ultimate load
(b) Slope deflection equations
(c) The principle of continuity at "last hinge"

The last hinge to form can either be obtained by an elastic-plastic analysis of a step-by-step formation of hinges, or by the assumption that each hinge in the structure in turn is the last to form. The correct deflection at ultimate is the maximum value obtained from the various trials.

Examples on the computation of vertical centerline deflections (fixed end beam with loading as shown):

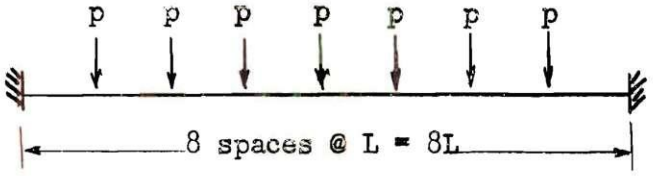

Fig. 17

Moment diagram:

Fig. 18

Mechanism:

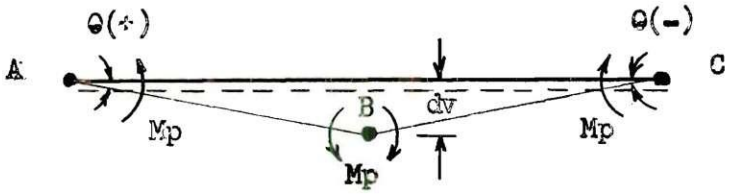

Fig. 19

Ultimate load:

$$P = \frac{Mp}{4L} \tag{58}$$

$$-MF_{AB} = MF_{BA} = MF_{BC} = -MF_{CB} \tag{59}$$

$$= \frac{4pL}{8} + \frac{pL(9L^2)}{16L^2} + \frac{pL^2(3L)}{16L^2} = \frac{20pL}{16} = \frac{5p}{2} \tag{60}$$

The slope deflection is used in this form as outlined in Neal (2):

$$\emptyset AB = \frac{d}{L} + \frac{L}{6EI}\left[2(M_{AB} - MF_{AB}) - (M_{BA} - MF_{BA})\right] \tag{61}$$

Then:

$$\emptyset AB = \frac{dv}{4L} + \frac{4L}{6EI}\left[(-2Mp + 5p) - (-Mp - \frac{5p}{2})\right] \tag{62}$$

$$\emptyset BA = \frac{dv}{4L} + \frac{4L}{6EI}\left[(-2Mp - 5p) - (-Mp + \frac{5p}{2})\right] \tag{63}$$

$$\emptyset BC = -\frac{dv}{4L} + \frac{4L}{6EI}\left[(2Mp + 5p) - (Mp - \frac{5p}{2})\right] \tag{64}$$

$$\emptyset CB = -\frac{dv}{4L} + \frac{4L}{6EI}\left[(2Mp - 5p) - (Mp + \frac{5p}{2})\right] \tag{65}$$

A hinge is considered positive if it causes extension of the fibers adjacent to the dotted line and conversely is considered

negative if it causes contraction of the fibers adjacent to the dotted line. The term "Ψ" is defined as the total rotation of a hinge, not to be confused with "θ", the rotation of the chord relative to the fixed end. Then we have:

$$\Psi_1 = - \phi AB \tag{66}$$

$$\Psi_2 = \phi BA - \phi BC \tag{67}$$

$$\Psi_3 = \phi CB \tag{68}$$

$$\Psi_1 = - \frac{dv}{4L} + \frac{4LMp}{6EI} - \frac{4L(15p)}{2(6EI)} \tag{69}$$

$$\Psi_2 = \frac{dv}{4L} - \frac{4LMp}{6EI} + \frac{4L(15p)}{2(6EI)} + \frac{dv}{4L} - \frac{4LMp}{6EI} - \frac{4L(15p)}{2(6EI)} \tag{70}$$

$$\Psi_3 = - \frac{dv}{4L} + \frac{4LMp}{6EI} - \frac{4L(15p)}{2(6EI)} \tag{71}$$

The last hinge to form is at B (Fig. 19), for the value of the deflection is the largest. Then we have:

$$\Psi_2 = \frac{dv}{2L} - \frac{4LMp}{3EI} = 0 \tag{72}$$

And:

$$dv = \frac{8MpL^2}{3EI} \tag{73}$$

Substituting the value of "dv" in Eqs. (69), (70), and (71), we get:

Ψ_1	Ψ_2	Ψ_3	(satisfies continuity)
-	0	-	

Gable frames: -- An example on the computation of the vertical deflection of the apex of a pitched gable frame follows:

Loading diagram:

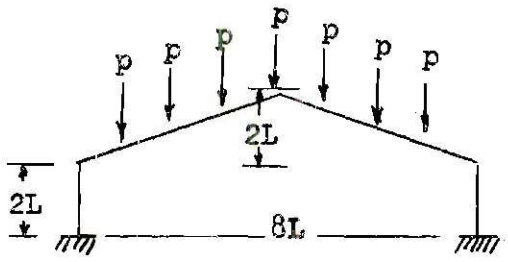

Fig. 20

Moment diagram:

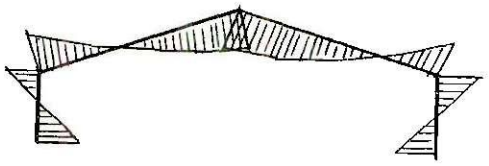

Fig. 21

Mechanism:

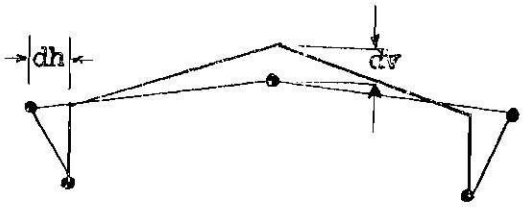

Fig. 22

Ultimate load:

$$Mp\theta\ (k_1 + 2k_2 + k_3) = pL\theta\ (8) \qquad (74)$$

$$p = \frac{Mp}{8L}\ (k_1 + 2k_2 + k_3) \qquad (75)$$

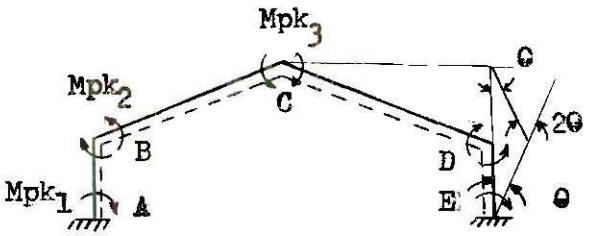

Fig. 23

Using the slope deflection equation:

$$-MF_{AB} = MF_{BA} = 0 \tag{76}$$

$$-MF_{BC} = MF_{CB} = \frac{5p}{2} \tag{77}$$

$$\emptyset AB = -\frac{dh}{2L} + \frac{2L}{6EI}\,(2Mpk_1 - Mpk_2) \tag{78}$$

$$\emptyset BA = -\frac{dh}{2L} + \frac{2L}{6EI}\,(2Mpk_2 - Mpk_1) \tag{79}$$

$$\emptyset BC = \frac{dv}{4L} + \frac{4L}{6EI}\left[(-2Mpk_2 + 5p) - (-Mpk_3 - \frac{5p}{2})\right] \tag{80}$$

$$\emptyset CB = \frac{dv}{4L} + \frac{4L}{6EI}\left[(-2Mpk_3 - 5p) - (-Mpk_2 + \frac{5p}{2})\right] \tag{81}$$

From Table 4:

$$k_1 \approx 1 \qquad k_2 \approx 1 \qquad k_3 \approx 1 \tag{82}$$

From the instantaneous center analysis:

$$dv = 4L\theta$$

$$dh = 2L\theta$$

$$dv = 2dh \tag{83}$$

The values of "Ψ" then are:

$$\Psi_1 = \phi AB = -\frac{dh}{2L} + \frac{2L}{6EI}(Mp) \tag{84}$$

$$\Psi_2 = \phi BC - \phi BA = \frac{dv}{4L} - \frac{4L(Mp)}{6EI} + \frac{4L}{6EI}\left(\frac{15p}{2}\right) + \frac{dh}{2L} - \frac{2L(Mp)}{6EI} \tag{85}$$

$$\Psi_3 = \phi CB = -\frac{dv}{4L} + \frac{4LMp}{6EI} \quad \frac{4L}{6EI}\left(\frac{15p}{2}\right) \tag{86}$$

The last hinge to form is at C (Fig. 23) since it gives the maximum value of deflection and still fulfills the principle of continuity. Then:

$$dv = 4L\left(\frac{4L}{6EI}\right)(Mp + 7.5p) \tag{87}$$

Substituting the values of "dv" and "dh" in Eqs. (84) and (85):

Ψ_1	Ψ_2	Ψ_3	(88)
-	+	0	

From Eqs. (67) and (74):

$$p = \frac{Mp}{2L} \tag{89}$$

Substituting the value of "p" in Eq. (87):

$$dv = \frac{16L^2}{6EI}\left(Mp + \frac{7.5Mp}{2L}\right) \tag{90}$$

Substituting the numerical values of L, E, I, and Mp from Tables 1 and 2:

$$dv = \frac{64 \times 52.5}{6 \times 30 \times 103} + \frac{64 \times 7.5 \times 52.5}{6 \times 30 \times 103 \times 4}$$

$$dv = 0.51 \text{ in.} \tag{91}$$

The proposed method of solution: -- The procedure to determine both the effects of axial thrust and deflections on gable frames is:

1. Determine the locations of possible plastic hinges
2. Select possible mechanisms
3. Set up the equation expressing the principle of virtual work:
   External work (W_E) = Internal Work (W_I)
4. Select the lowest critical load to cause failure which in turn yields the correct mechanism
5. Check equilibrium by drawing moment diagram
6. Moments are now all known. By statics solve for axial load on members of the structure.
7. Apply the interaction formula to find the values of k_1, k_2, and k_3
8. Solve for the deflection at "ultimate"
9. Take the new configuration of the structure prior to failure and compute the critical load as in step 4. This should be ample to give a conservative value of the ultimate load.
10. If a more precise analysis is required, knowing the new critical load, repeat steps 5, 6, and 7 and find the new deflection associated with the new critical load and repeat step 4. These repetitions will converge to the exact answer.

For gable frames, Types I and II: -- The equation below gives the ultimate load for the different ratios of span-to-rise and to height of columns:

$$p = (0.125 + R\,\frac{h}{L})\,Mp \qquad (92)$$

Where R is a constant:

For the height of column of "2L", R = 0.25
For the height of columns of "L", R = 0.50

The results are shown in Figs. 57 and 58.

To modify for deflection, the equation becomes:

$$p = \left[0.125 + R\left(\frac{h - d}{L}\right)\right] Mp \qquad \text{when } h > d \qquad (93)$$

and:

$$p = (0.125)\, Mp \qquad \text{when } h \leq d \qquad (94)$$

The results of the above equations are also given in Figs. 57 and 58.

CHAPTER III

DESCRIPTION OF TESTS

All test specimens were loaded in an Olsen, screw-powered constant strain machine of 20,000 lbs. capacity, reading to the nearest 0.2 lbs. Increments of load were varied, depending on the ultimate load capacity of the specimens. The objective was to get an indicative load-deformation curve. This type of machine was chosen to avoid any dynamic effect and to speed testing.

Test Arrangement: -- The test arrangement is shown in Fig. 25. The specimens were mounted on a 24" x 30" x 3/4" plywood board by 4" x $\frac{1}{2}$" x 0'-4" steel plates with a 3/16" keyway in which the legs of the model were set. Small 2" x $\frac{1}{4}$" x 0'-1$\frac{1}{2}$" plates locked the legs firmly to the steel plates with two $\frac{1}{4}$" bolts. In turn, the 4" x $\frac{1}{2}$" x 0'-4" steel plates were fastened to the plywood board with four $\frac{1}{4}$" carriage bolts. The plywood board was set on two 2" x 4" x 16" pieces of lumber in a vertical position and was braced with two 2" x 2" x 20" pieces of lumber to insure its stability. The two 2" x 4" x 16" pieces of lumber formed the base of the plywood board. The base of the plywood board was set on two $\frac{1}{4}$" x 3$\frac{1}{2}$" x 16" flat plates welded to four vertical 1$\frac{1}{2}$" steel pipes 24" long. In turn, the pipes were fastened to a 20" x 20" x $\frac{1}{2}$" plywood base.

The movable head of the testing machine was set under the 3/4" plywood board on which the model was fastened and between the two rows of $1\frac{1}{2}$" steel pipes, thus allowing the head to move up and down freely below the model.

Assembly of Test Specimens: -- The load was transmitted to the model by a series of loading beams connected with flexible U-shaped brass clevises having needle point hardened steel screws to allow transverse movement. A detail of the clevises is shown in Figs. 28 and 29. The spreader beams were connected to the model by tension rods of definite lengths to follow the contour of the model. The rods were screwed to both the clevises attached to the beams and to similar steel clevises attached to the model. The load from the machine head to the beams was transmitted through a $\frac{1}{4}$" aluminum rod connected by a clevis to the loading beam at one end and having a 6" x $\frac{1}{4}$" x 0'-6" aluminum plate on the other, to which pressure was applied by the testing machine's moving head. The dead weight of the loading assembly was ten pounds.

Material: -- The material used for the tests was taken from hot rolled 3/16" x 3/16" x 12'-0" long rods. Pieces 12" long were cut and placed in an oven at 1400° F. for eight hours, then allowed to cool slowly over a period of 16 hours. The purpose of annealing the steel was to relieve any residual stress that could have occurred in the manufacturing process and to eliminate as much as possible the effect of heat generated from welding the members in making the model. A number of coupons were tested to establish "Mp" (the plastic moment) and the

physical characteristics of the material. The material exhibited characteristics similar to those of ordinary A-7 steel.

Instrumentation: -- Schematic drawings of the instrumentation used for Types I and II are shown in Figs. (a) and 27(b). Type III is shown in Fig. 29(c). The simple beam tests are shown in Fig. 29(e), and the portal frame (P-1) is shown in Fig. 29(d).

The vertical deflections were measured with the plunger of the micrometer dial inserted between the U-shaped clevis bearing directly on the upper part of the model. The horizontal deflections were measured by having the plunger bear on the side of the model where the deflections were desired.

For Type III, micrometer gage dials were placed on the end blocks to detect any horizontal movements of the bases. The dial gages were bolted to angles which were either bolted or clamped to the 3/4" plywood board base.

The Coupon Test: -- Two coupons of the annealed specimens were subjected to a tension test. A hydraulic testing machine with an extensometer and an electronic recorder were used to determine the variation in yield strength. The results of the tests are tabulated in Table 2.

Test Procedure: -- The 4" x $\frac{1}{2}$" x 0'-4" steel blocks serving as the base were set in the proper position and securely fastened to the 3/4" plywood board base. The model was inserted in the 3/16" keyway and locked in place.

The clevises that transmit the load to the loading beams were screwed to the model, and the micrometer dial gages were set at the desired locations, as shown in Fig. 27.

The table on which the model assembly rests was set on the testing machine. The movable head of the machine was lowered to clear the top of the table. The model assembly was set on the table allowing the $\frac{1}{4}$" rod that transmits the load to the loading beams to pass through the movable head, and a 6" x 6" plate was inserted and bolted to the rod below the movable head of the testing machine. The force was thus transmitted to the model as the head moved down.

Increments of load were applied to the model allowing a time lapse of two to ten minutes between successive loadings. As the load approached the ultimate capacity of the model, a greater loss of load was observed even though the strain was held constant. Ample time was given for the loads to settle before additional strains were applied. Readings of the minimum loads and the deflections associated with these loads were recorded. The primary purpose of these tests was to determine:

1. The ultimate load at collapse
2. The deflections at collapse

The results of these tests are shown in Figs. 32 to 59, inclusive.

CHAPTER IV

TEST RESULTS

Vertical Deflections

Types I and II: -- The vertical deflections of the apex in all cases indicated clearly the point at which the structure collapsed.

Due to imperfections in the model itself and in the method of testing, the locations of the hinges at the weld points were formed outside the welds since the "Mp" of the welds was slightly higher than the "Mp" of the section. This factor created a local effect but did not affect the ultimate load of the model appreciably.

In all cases except Types I-6, I-7, II-6, and II-7, where the welds at the apex extended a distance of about one half inch, the hinges were formed under the load adjacent to the apex and the ultimate load was higher than predicted, as shown in Figs. 37, 38, 44, and 45.

The deflections measured were slightly less than the calculated deflections except in Types I-6, I-7, II-6, and II-7, namely for the reasons outlined below:

1. The load at collapse was less than the load predicted by the simple theory
2. Strain hardening does occur, thus reducing deflections at ultimate load
3. Imperfections were present in the making of the model

Eqs. (93) and (94) enable us to predict within a limit of accuracy the ultimate load of the structure. A summary of all results is shown graphically in Figs. 57 and 58.

Type III: -- The deflections were measured in the same manner as for Types I and II. The deflection of the apex of the model defined clearly the point at which failure occurred. The ultimate load of the structure was much lower than the predicted ultimate load by the simple plastic theory because the deflections have considerable effect on the reduction of the "plastic moment" due to increase of axial load and change of geometry of the structure.

This deflection effect becomes very critical in low rise-to-span ratios and a reduction of 50% from the predicted ultimate load by the simple theory was observed in tests. The results of all the tests are plotted in Fig. 59 and compared with the theoretical results from the simple plastic theory. The percent reductions due to the effect of deflections are shown in Table 6.

Portal Frame - Type P-1: -- The vertical deflection showed clearly the point at which failure occurred. A 3/8" long weld extended in the region where the last hinge was supposed to form. Catenary action caused the movement of the columns of the frame. A collapse mechanism in the manner shown in Fig. 24 was formed which yielded a higher ultimate load and a greater deflection than that predicted. The results are shown in Fig. 54.

The object of this test was to determine the "Mp" of the welds. It is of interest to know that the "Mp" of the welds was greater than that of the section. The calculations are shown on the following page.

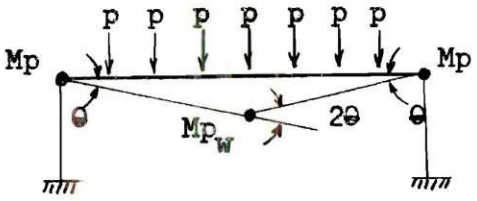

Fig. 24

$$2\theta\ (Mp + Mp_w) = 2pL\theta\ (1 + 2 + 3 + 2) \tag{95}$$

$$Mp_w = 8pL - Mp \tag{96}$$

$$Mp_w = 116 - 51.5 = 65.5 \tag{97}$$

$$Mp_w = 1.26\ Mp \tag{98}$$

Simple Beams - Types B-1 and B-2: -- The objective of these tests was to substantiate the value of "Mp" obtained from the coupon tension test. The vertical deflection was obtained from the micrometer gage readings and it defined clearly the point at which collapse occurred. (See Figs. 55 and 56). The test was extended to show the regions where strain hardening started. The value of "Mp" in the beam tests agrees with the calculated value from the coupon tests and the results are shown in Table 3.

Types I and II: -- The measuring of the horizontal deflections was not too significant. It was of interest to find that as the plastic moment was developed at the base of the columns, the structure started moving to one side. This was due to imperfections in the model itself and in the testing equipment. Since the horizontal deflections were not indicative of failure, they were plotted for only Types I-1 and II-1 in Figs. 32 and 39.

Type III: -- The intent of measuring the horizontal deflections was to detect any movement in the blocks that served as the base of the model. The movement was in the order of 0.001" to 0.002" and can be neglected.

Portal Frame - Type P-1: -- The horizontal deflections were significant for they gave a good indication as to when catenary action started and showed the movement of the columns. (See Fig. 54).

Beams - Types B-1 and B-2: -- The horizontal deflections of the ends were not measured.

Material Properties

Coupons: -- A hydraulic testing machine with an extensometer and an electronic recorder was used in the tests. The yield strength of the two specimens tested was very close and the average of the tension test results was used in the calculation of "Mp", the plastic moment. Results of these tests are shown in Table 2.

CHAPTER V

DISCUSSION AND CONCLUSIONS

The theory developed for the solution of the ultimate load of gable frames proved to be adequate. The proposed method is outlined below:

1. Determine the location of possible hinges
2. Select possible mechanisms
3. Set up the equation expressing the principle of virtual work:
   External Work, "W_E" = Internal Work, "W_I"
4. Select the lowest critical load to cause failure which in turn yields the correct mechanism
5. Check equilibrium by drawing moment diagram
   $$M \leqslant Mp$$
6. Moments are now all known. By statics solve for axial load on members of the structure
7. Apply interaction formula to find the values of k_1, k_2, and k_3.
8. Solve for the deflection at "ultimate"
9. Take the new configuration of the structure prior to failure and compute the critical load as in step 4. This should be ample to give a conservative value of the ultimate load.

Effect of Axial Thrust

Types I and II: - One of the factors that will influence the reduction of "Mp" due to axial forces in the ratio of P/Mp, the greater

this ratio the smaller the "k" values and the greater is the reduction. This explains the fact that the greater the rise-to-span ratio, the greater was the reduction in Mp since P (the ultimate load) becomes greater.

In Type I-1 with a rise-to-span ratio of 1:4 and a ratio of P/Mp of 1.74, the "k" values were (see Table 4):

$k_1 = 0.998$ $k_2 = 0.998$ $k_3 = 0.999$

In Type I-7 having a rise-to-span ratio of 1:64 and a ratio of P/Mp of 0.89, the "k" values were:

$k_1 = 0.999$ $k_2 = 0.999$ $k_3 = 0.999$

In Type II-1 having a rise-to-span ratio of 1:4 and a ratio of P/Mp of 2.6, the "k" values were:

$k_1 = 0.996$ $k_2 = 0.995$ $k_3 = 0.998$

In Type II-7 having a rise-to-span ratio of 1:64 and a ratio of P/Mp of 0.97, the "k" values were:

$k_1 = 0.999$ $k_2 = 0.997$ $k_3 = 0.997$

Thus the effect of axial force on the reduction of "Mp" is not very critical when a square section is used, and when P/Mp is small an upper value of this ratio has not been established. In case a WF section is used, the reduction in "Mp" due to axial force becomes more critical and should be computed for each individual case.

A gable frame similar to Type I-1 with L = 5'-0" and 18WF50 members gave a ratio of P/Mp = 0.00835 and computed "k" values of:

$k_1 = 0.95$ $k_2 = 0.95$ $k_3 = 0.98$

Another frame similar to Type II-1, with similar characteristics as the previous frame, gave a ratio of P/Mp = 0.0125 and computed "k" values of (see Appendix C):

$k_1 = 0.89$ $k_2 = 0.87$ $k_3 = 0.95$

Type III: -- It is evident from the previous discussion that the ratio P/Mp is an important factor in the reduction of "Mp" and that this ratio is more critical for this type of structure than it is for gable frames. The use of WF sections in such a type of frame makes the reduction even greater. Contrary to the case for gable frames where the greater the rise-to-span ratio, the greater the axial thrust, it was observed in Type III that between the limits of rise to span of 1:4 to 1:64, the lower the rise, the greater the axial thrust. This stands to reason, since "P" as computed by the simple theory is constant.

The average values of "k" varied from 0.988 in the 1:4 rise-to-span ratio to 0.479 in the 1:64 rise-to-span ratio, yielding a reduction in ultimate load of 52% in the latter case. (See Table 5).

Effect of Deflections

Types I and II: -- It was obvious from the tests that the deflections had an effect on the ultimate load of the model. In Type I, this effect caused a reduction[1] of 4.4% in the 1:4 rise-to-span ratio (Type I-1) and 6% in the 1:9.4 rise-to-span ratio (Type I-4). The

---

[1] The reduction represents the deviation of test results from the simple plastic theory.

calculated reduction of the ultimate load due to deflection by the modified theory as compared to the simple theory, varied between 6.6% in the 1:4 rise-to-span ratio (Type I-1) and 8.4% in the 1:32 rise-to-span ratio (Type I-6)(see Table 5).

The effect of deflections in Type II caused a reduction (see fn. [1]) in ultimate load that varied between 7.4% in the 1:4 rise-to-span ratio (Type II-1) and 12.6% in the 1:16 rise-to-span ratio (Type II-5). The reduction calculated by the modified theory as compared to the simple theory varied between 11.2% in the 1:4 rise-to-span ratio (Type II-1) and 15.2% in the 1:32 rise-to-span ratio (Type II-6) (see Table 5 and Figs. 60 and 61).

The effect of deflections is reduced if a WF section is used to replace a square section because of the smaller shape factor ("f") of the WF section, as compared to a square section; i.e., a greater "I" as compared to that of a square section of the same moment carrying capacity. Roughly, the deflections of a WF frame, at "ultimate", would be $(\frac{1.14}{1.5}) \times 100\%$ of those for rectangular sections.

A comparison of the reduction[2] due to deflections between a rectangular section and a WF section if shown in Figs. 60 and 61 for Types I and II frames.

Type III: -- The deflections in such a type frame seem to be very important. Their effect on the ultimate load caused a reduction varying from 13% to 51% (see Table 6) and was most critical in Type III-7, where

---

[2] The reduction is based on the difference in "ultimate load" predicted by the simple plastic theory and the modified theory.

the rise-to-span ratio was 1:32. No solution was established to predict this effect because the configuration of the structure prior to collapse could not be determined.

CHAPTER VI

RECOMMENDATIONS

The following recommendations for improvements on the testing equipment should lead to more accurate results:

1. All similar models should be bent to the proper configuration, then annealed in an oven. Welds are a source of error if not performed properly by a qualified welder.

2. A system of turnbuckles on the tension rods that connect the loading beams to the model could be used to a greater advantage and would save time in setting up the test.

The following lines of study should prove rewarding for further investigation of gable frames:

1. More study could be made to establish the effect of "P/M_p" on frames with different spans, column heights, and rise-to-span ratios, having different type sections. Until such a relationship is established, each frame should be analyzed as a case in itself.

2. More research work could be done on Type III structures to determine the effect of deflections.

3. The effects of axial force and deflections in frames having members of variable sections should be investigated.

APPENDIX A

FIGURES

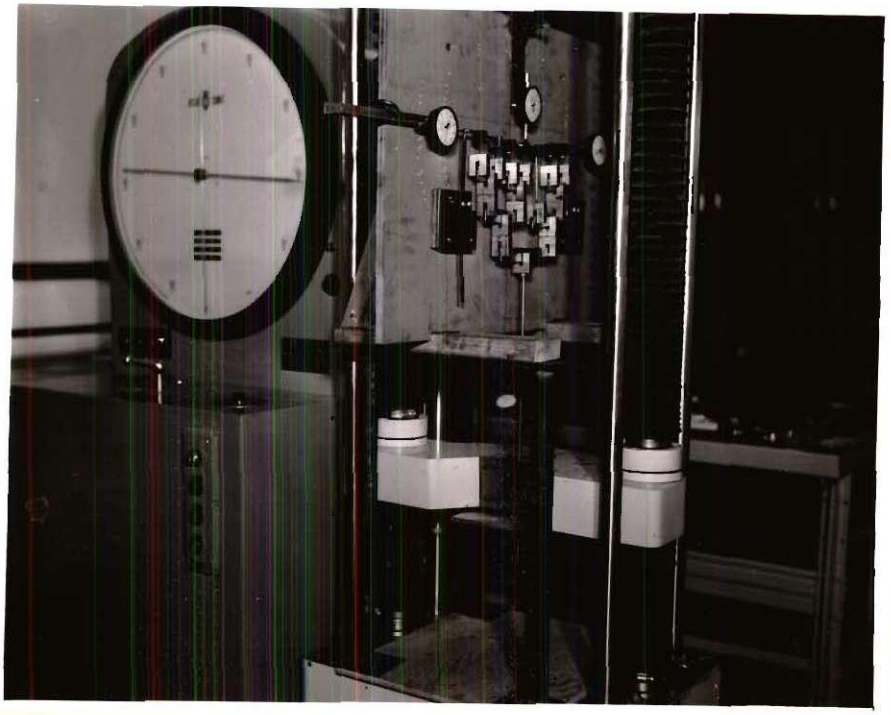

Fig. 25. Test Arrangement

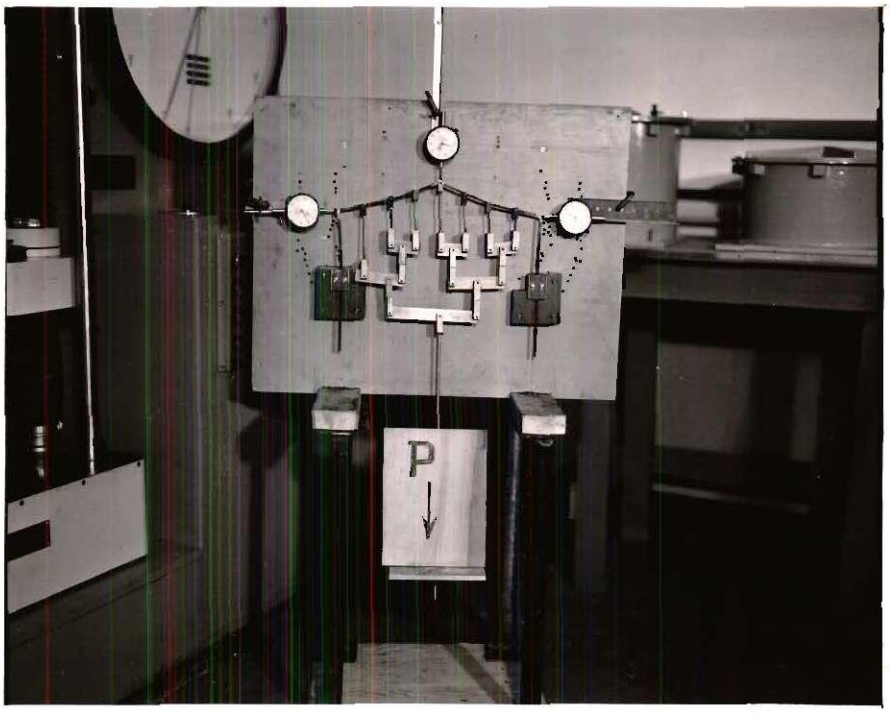

Fig. 26. Test Assembly

Type I

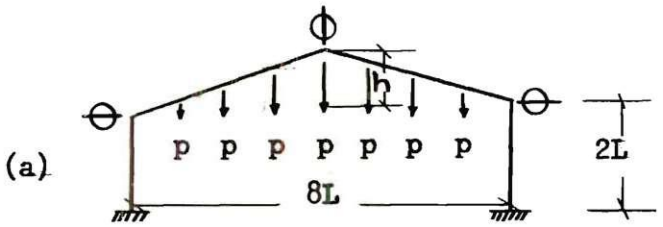

Type II

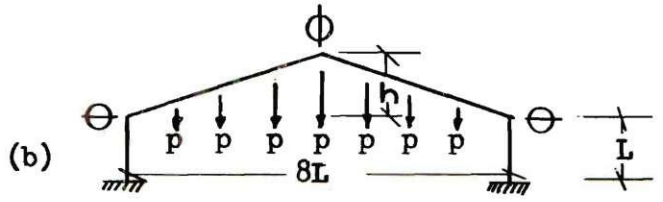

Type III

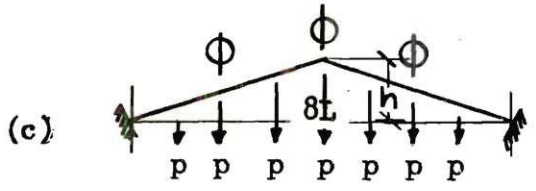

Type P-1

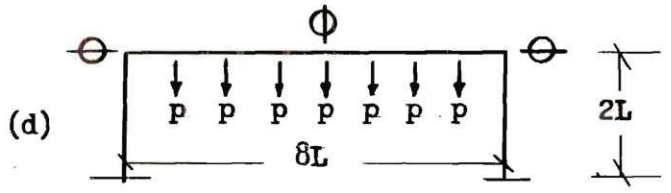

Types B-1 and B-2

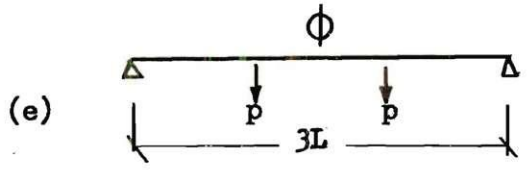

Note: For values of "L" and "h" see Table 1.

Fig. 27. Schematic Drawing of the Instrumentation and Type of Loading

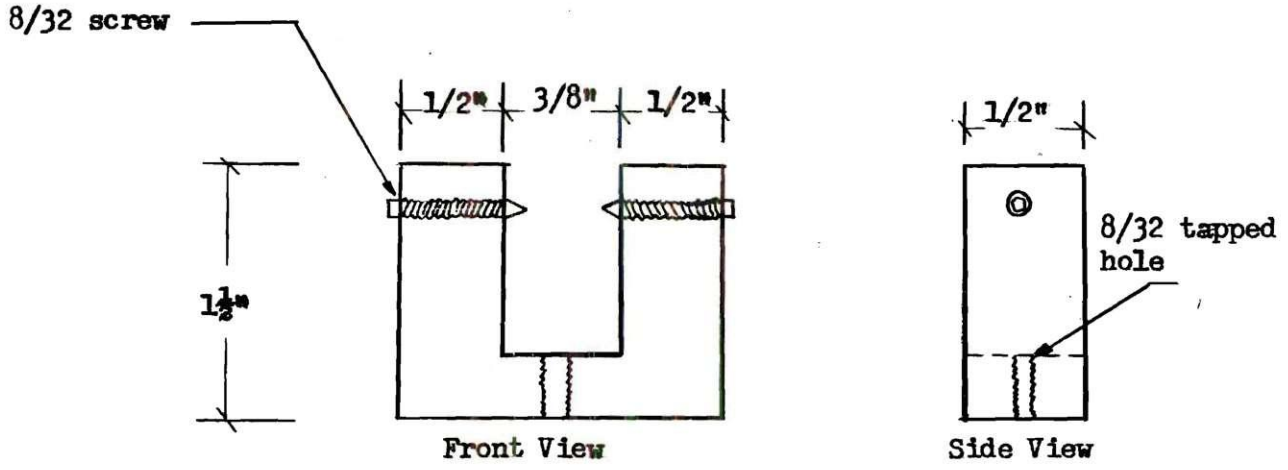

Fig. 28. Detail of Loading Beam Clevis

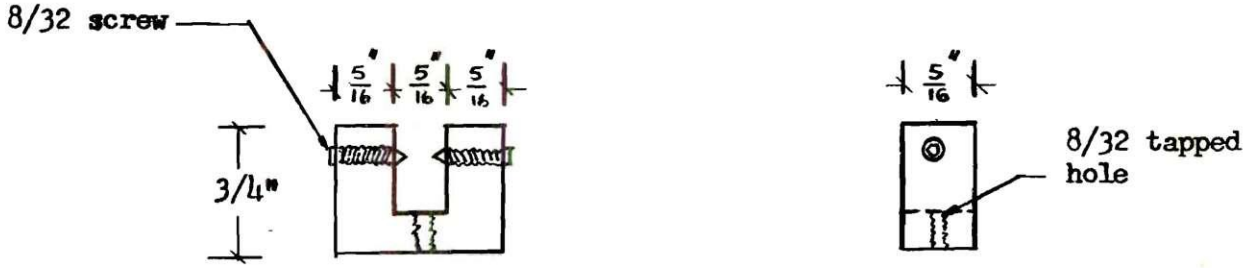

Fig. 29. Detail of Model Clevis

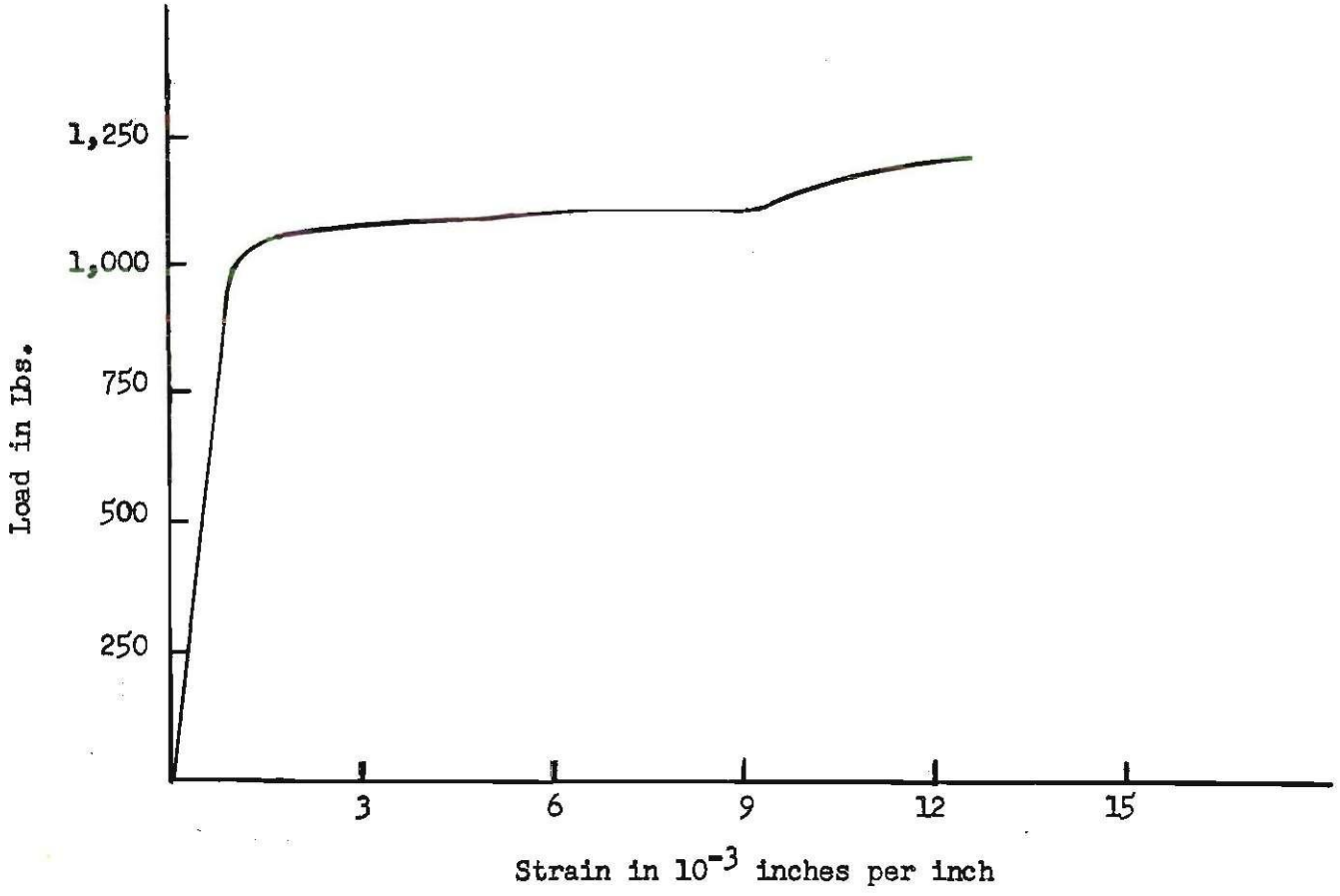

Fig. 30. Coupon Tension Test T-1

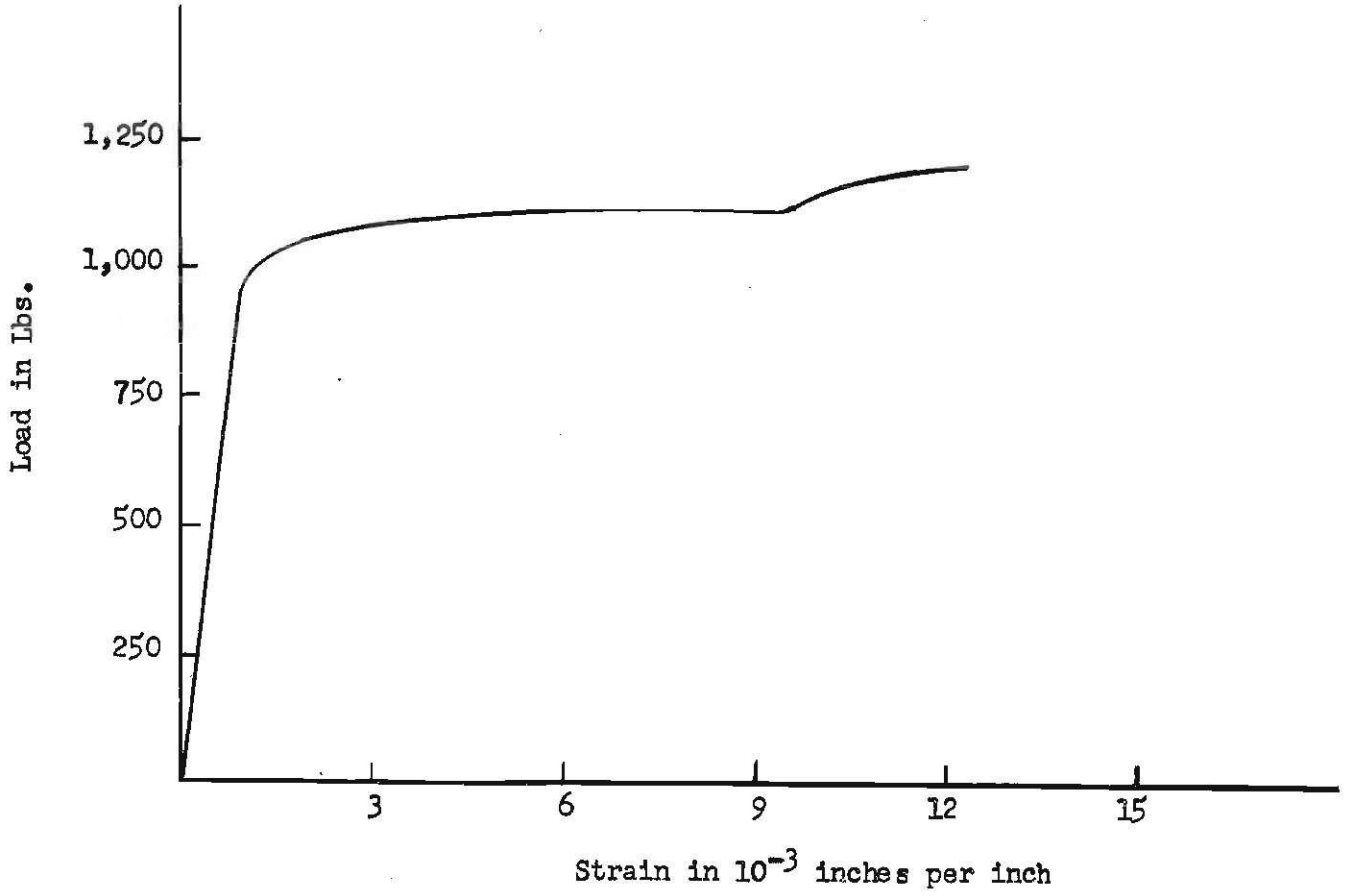

Fig. 31. Coupon Tension Test T-2

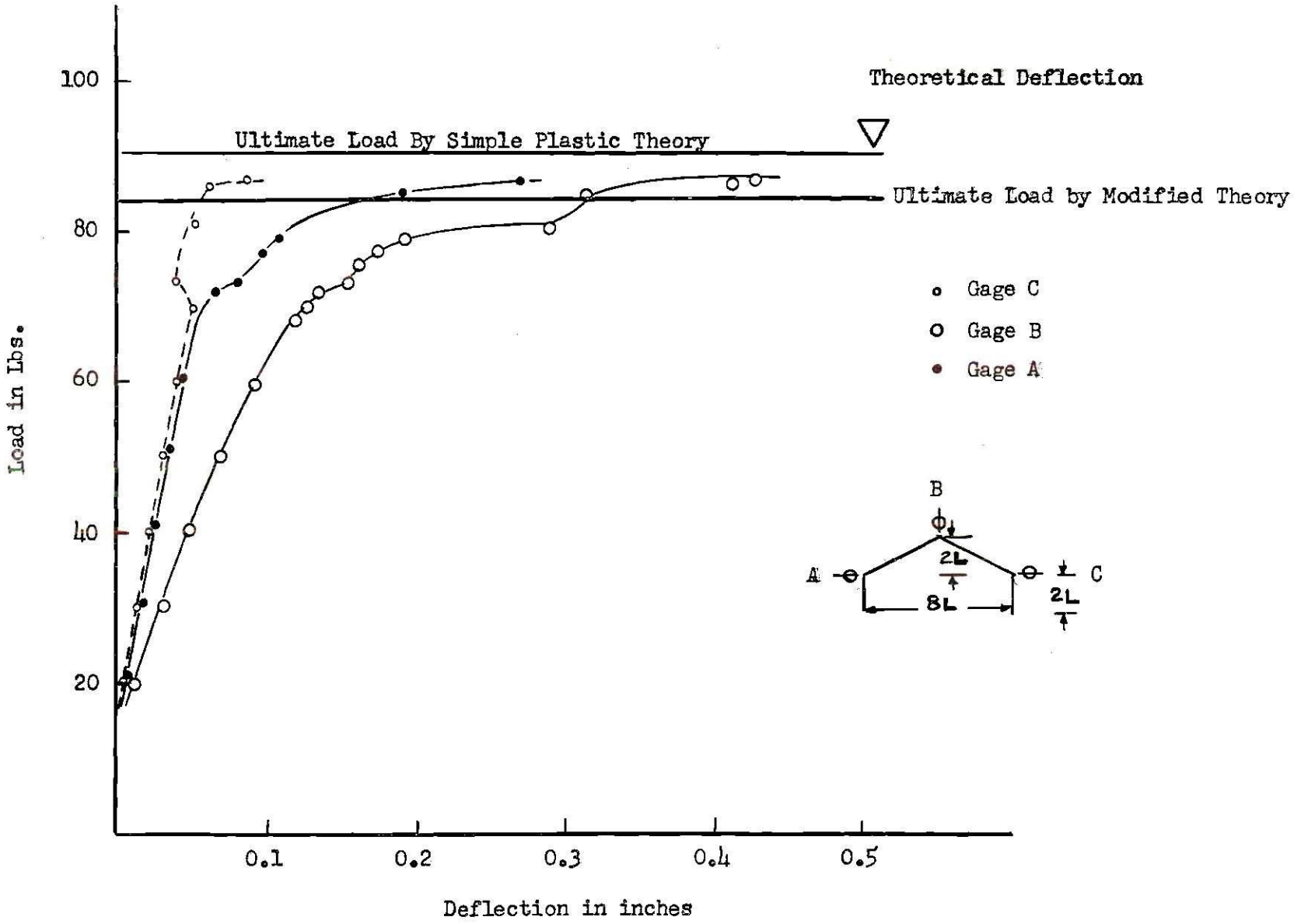

Fig. 32. Vertical and Horizontal Deflections for Test I-1

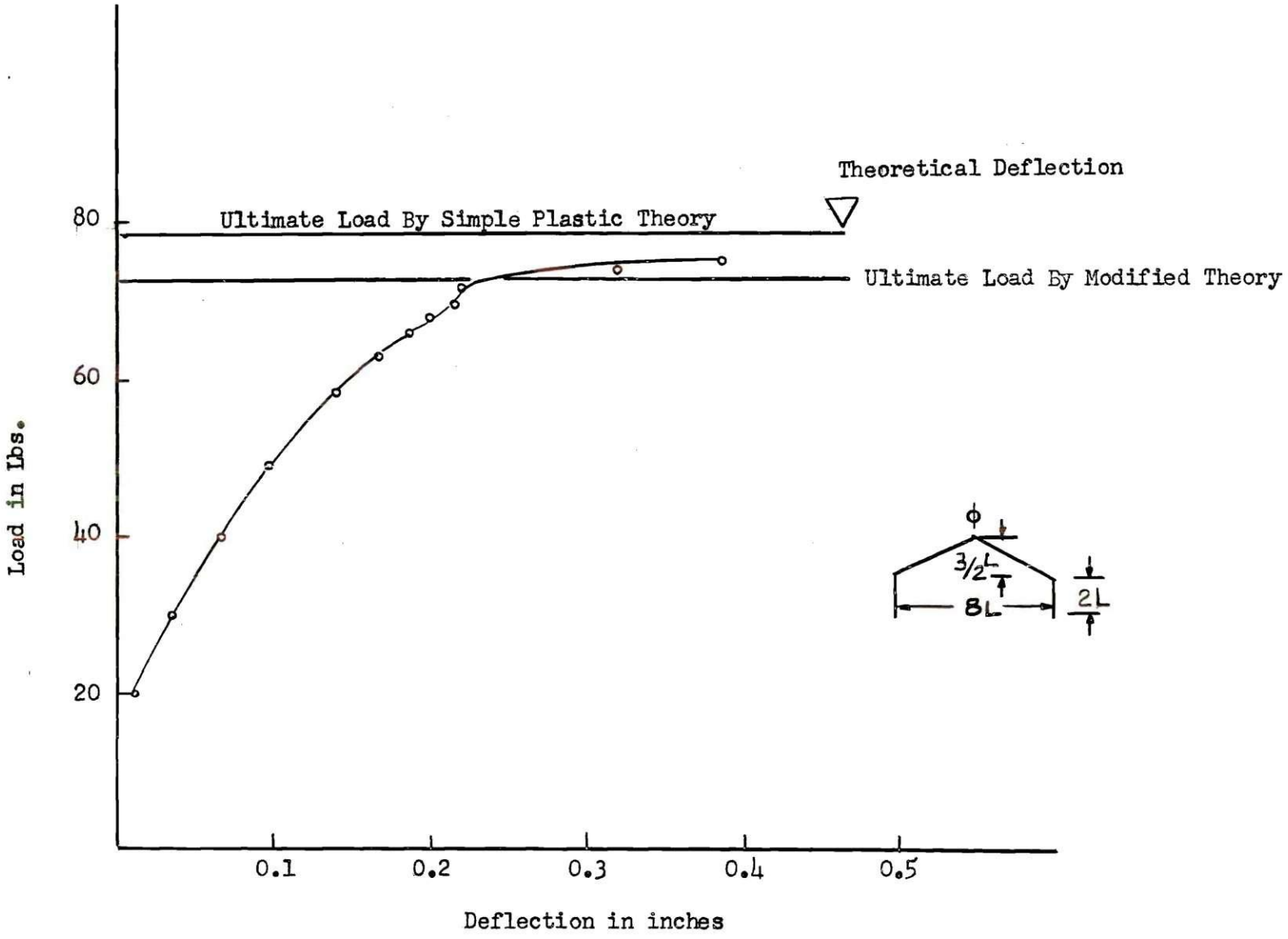

Fig. 33. Vertical Deflection of the Apex for Test I-2

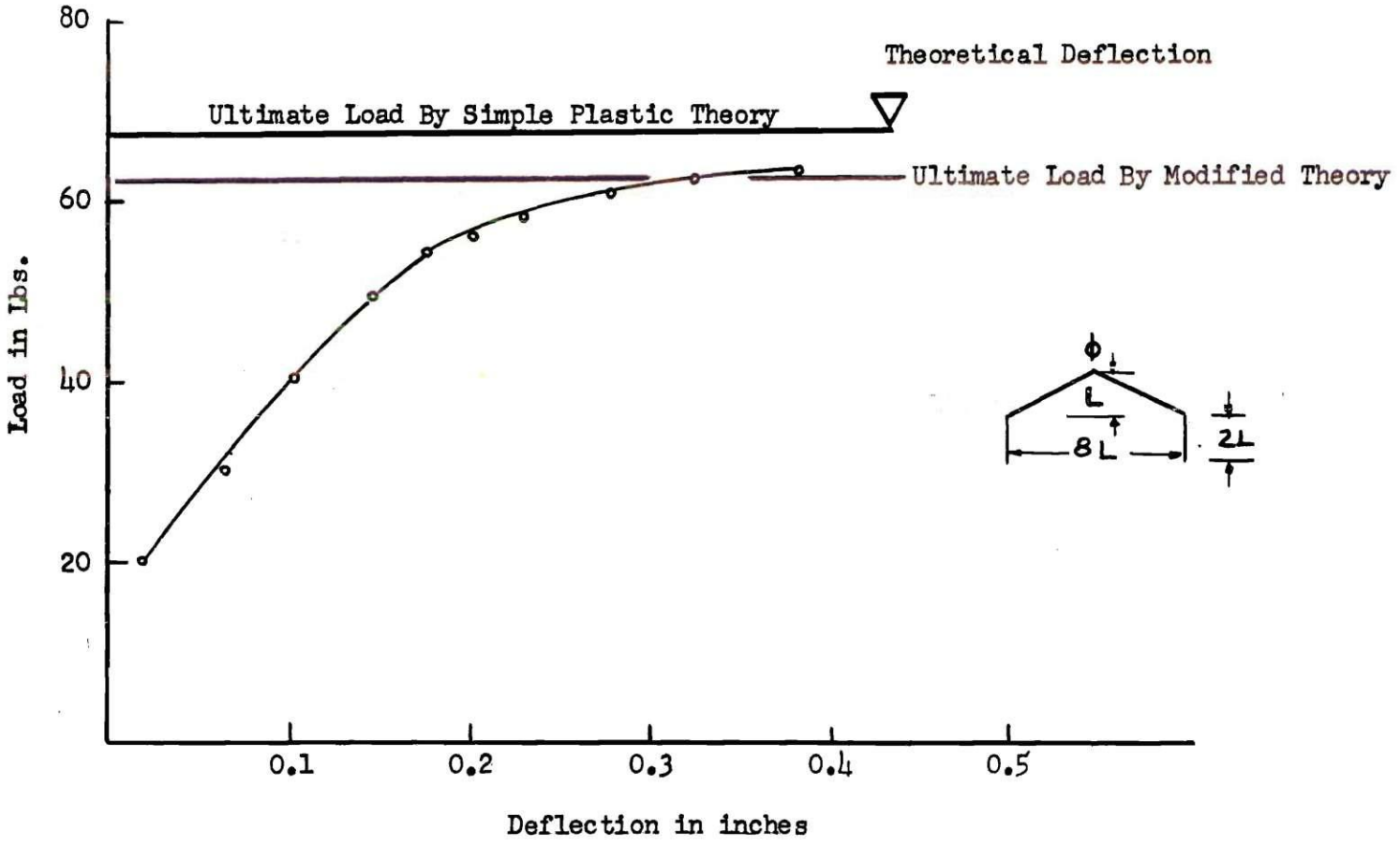

Fig. 34. Vertical Deflection of the Apex for Test I-3

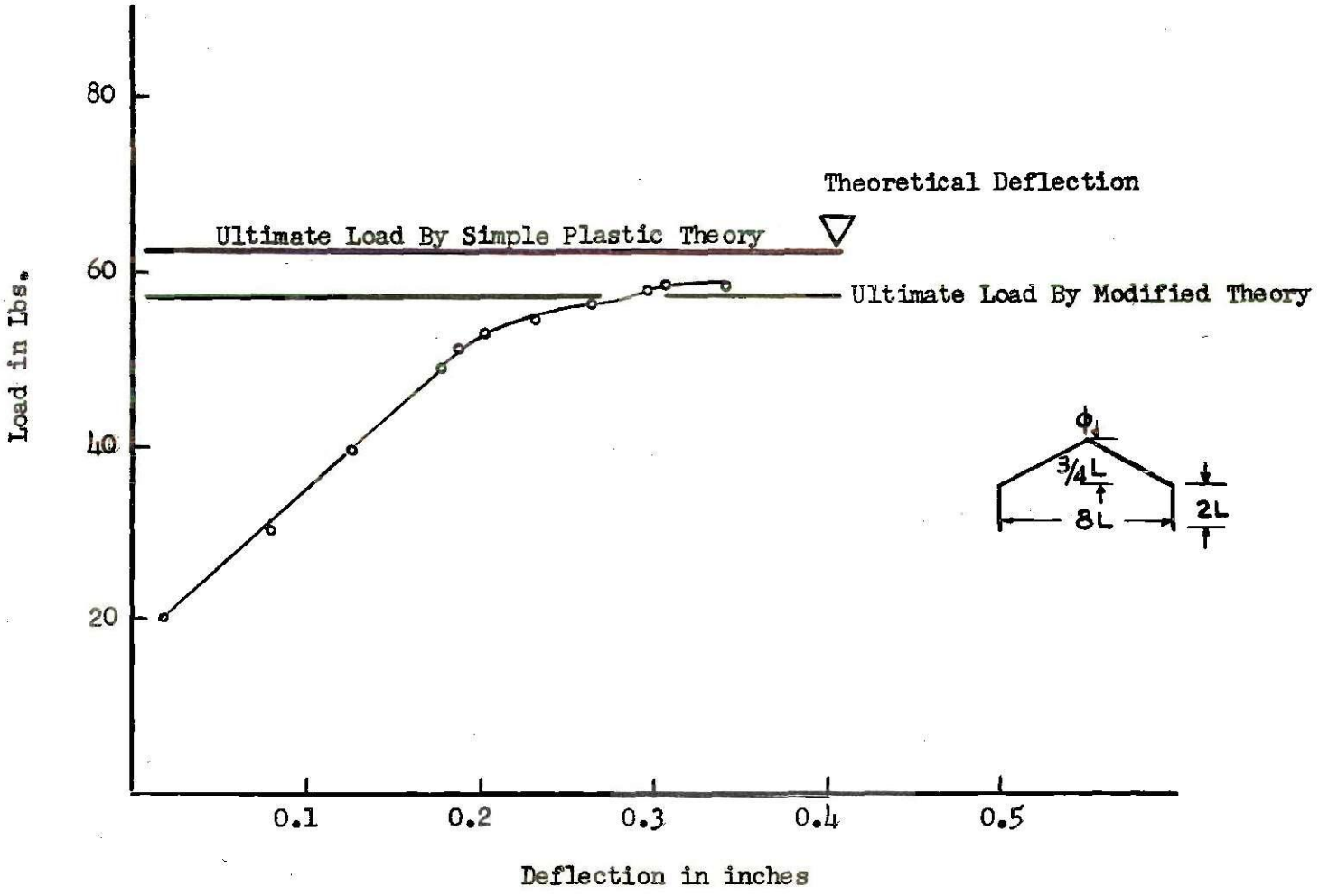

Fig. 35. Vertical Deflection of the Apex for Test I-4

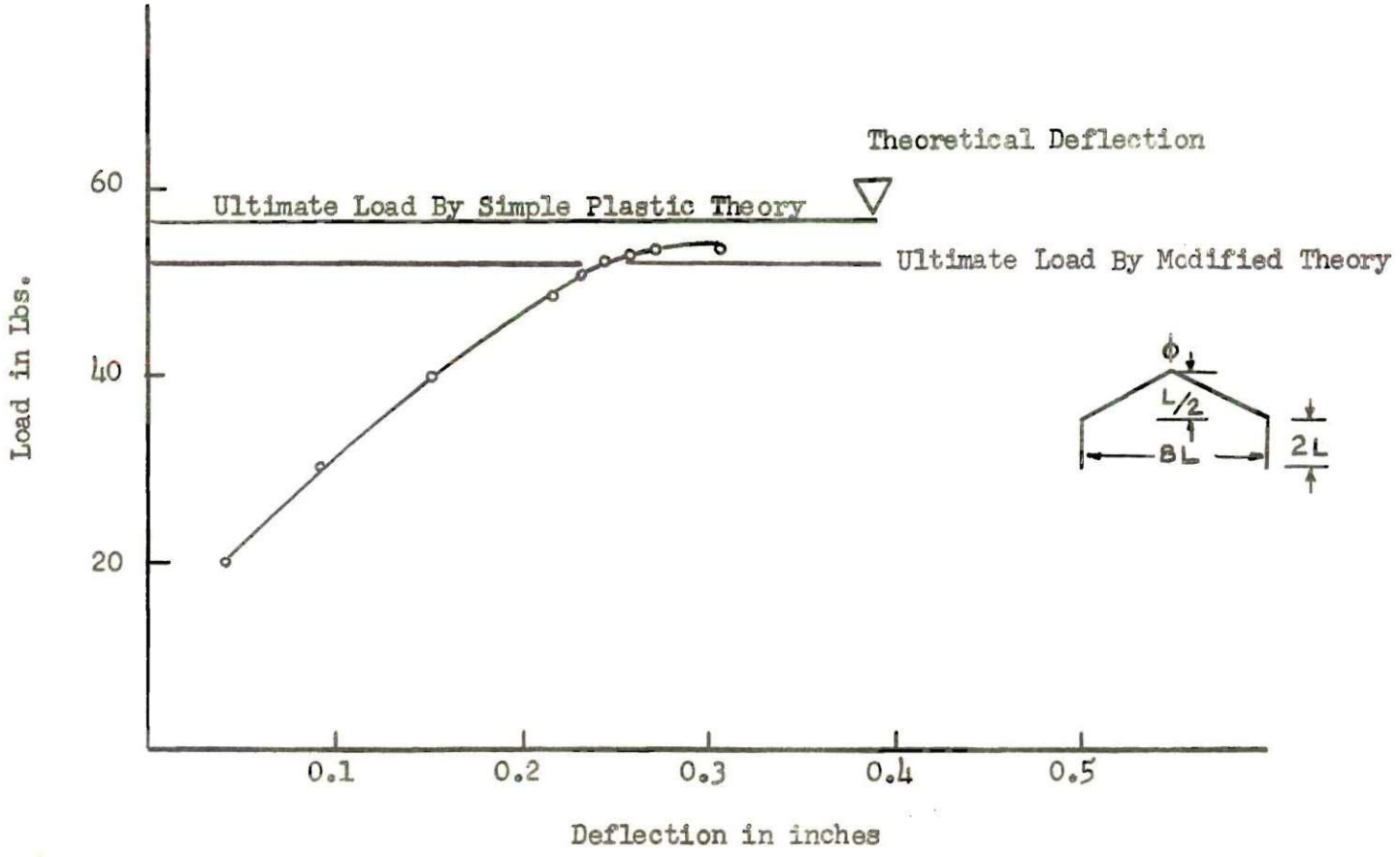

Fig. 36. Vertical Deflection of the Apex for Test I-5

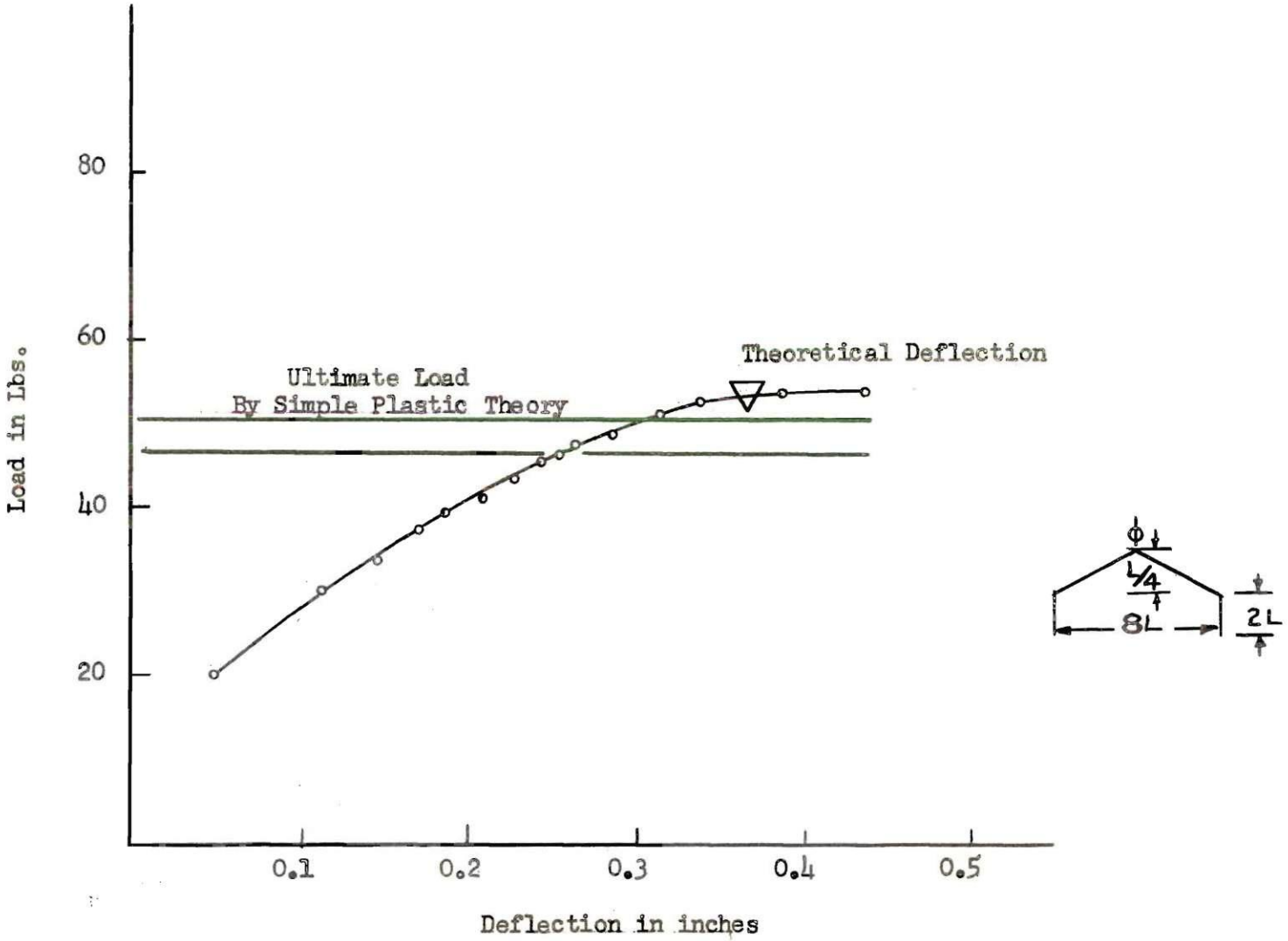

Fig. 37. Vertical Deflection of the Apex for Test I-6

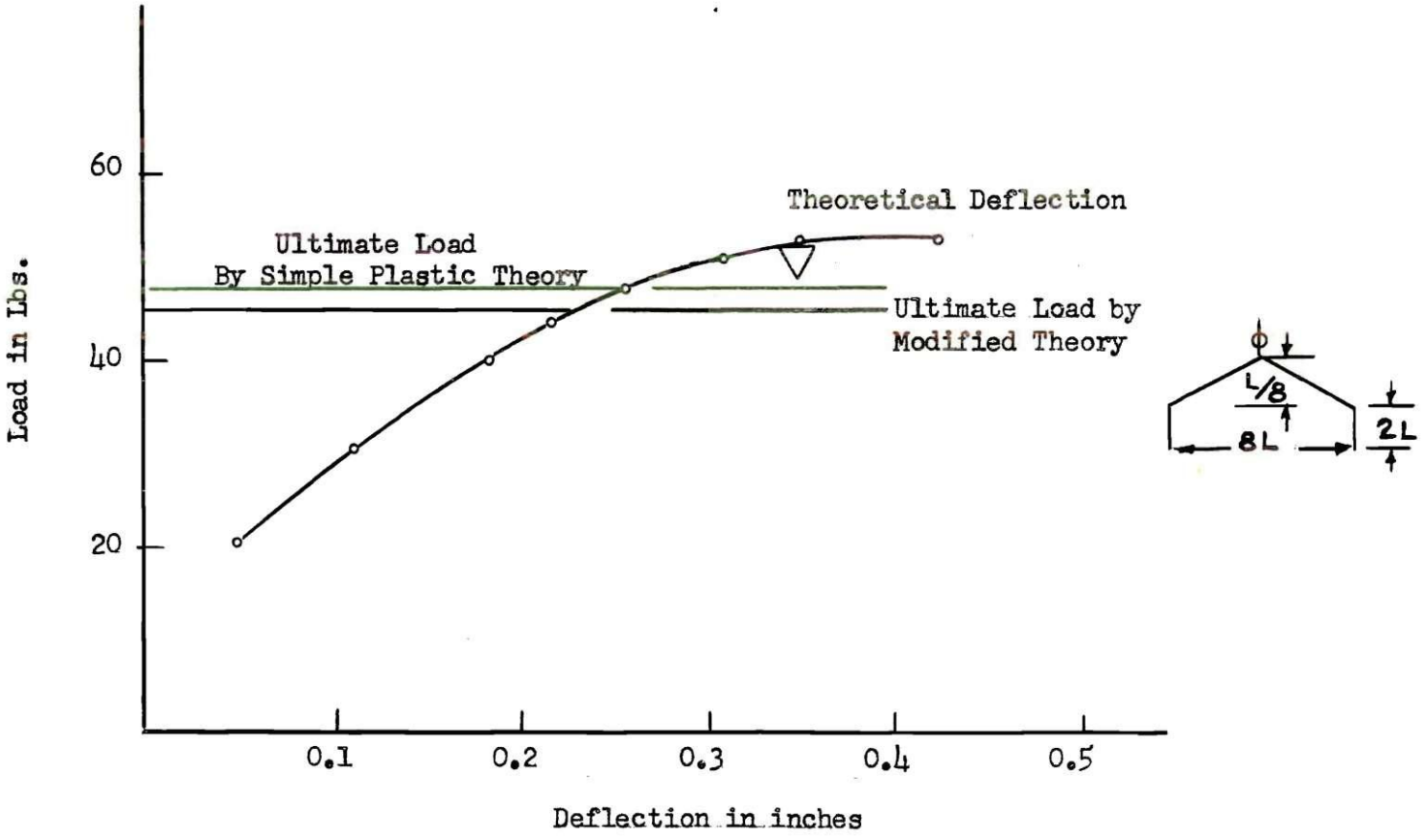

Fig. 38. Vertical Deflection of the Apex for Test I-7

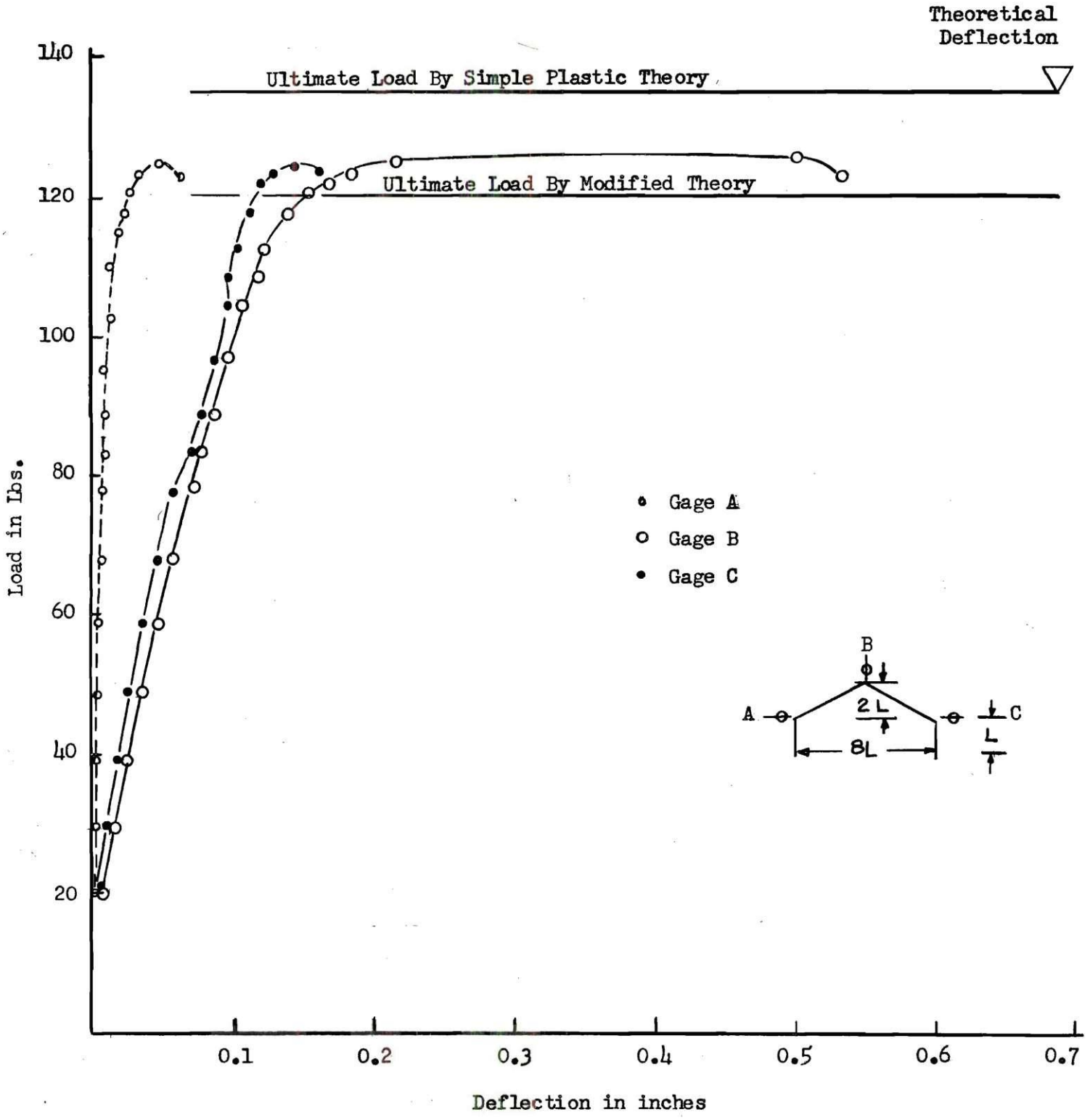

Fig. 39. Vertical and Horizontal Deflections for Test II-1

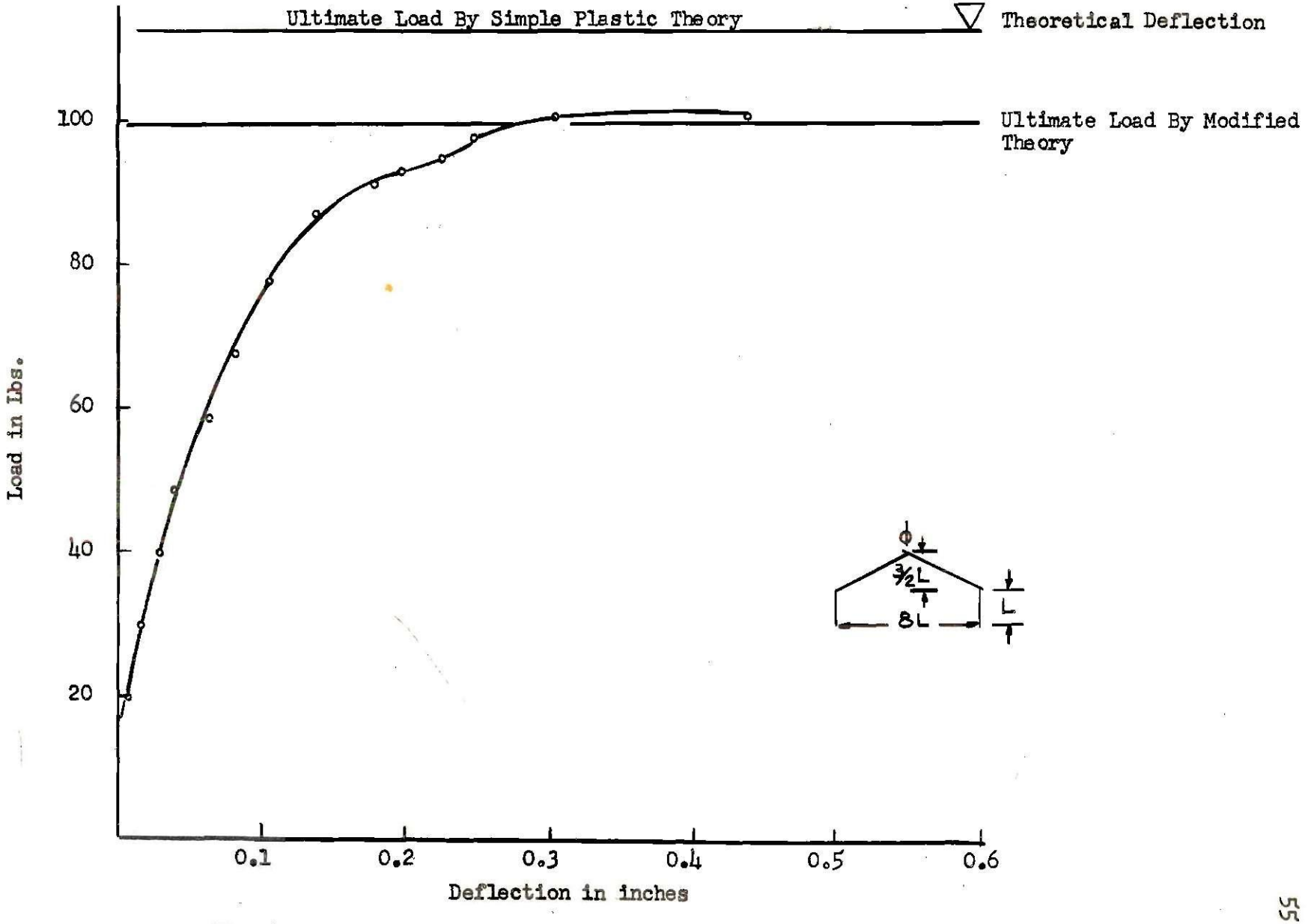

Fig. 40. Vertical Deflection of the Apex for Test II-2

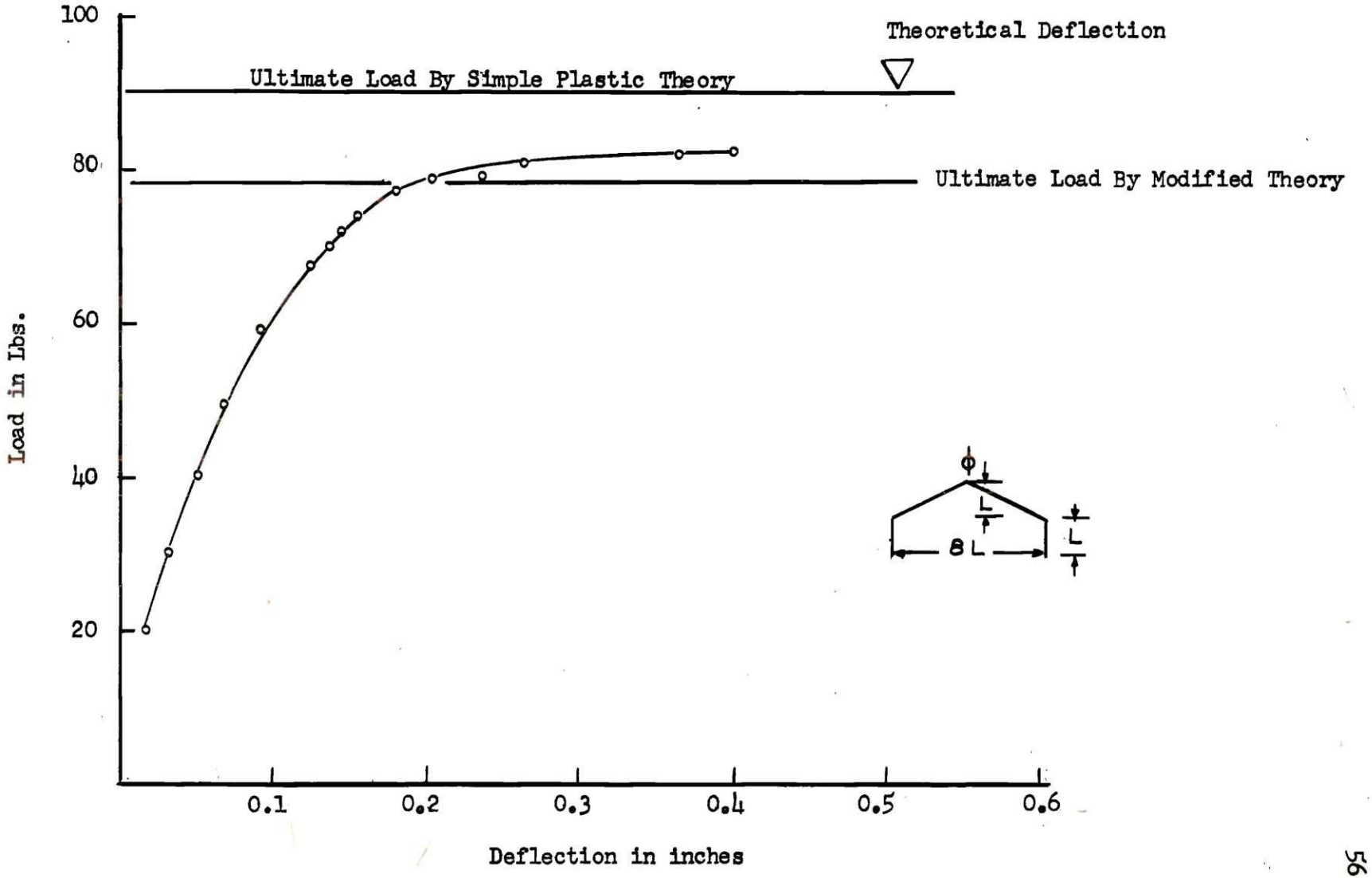

Fig. 41. Vertical Deflection of the Apex for Test II-3

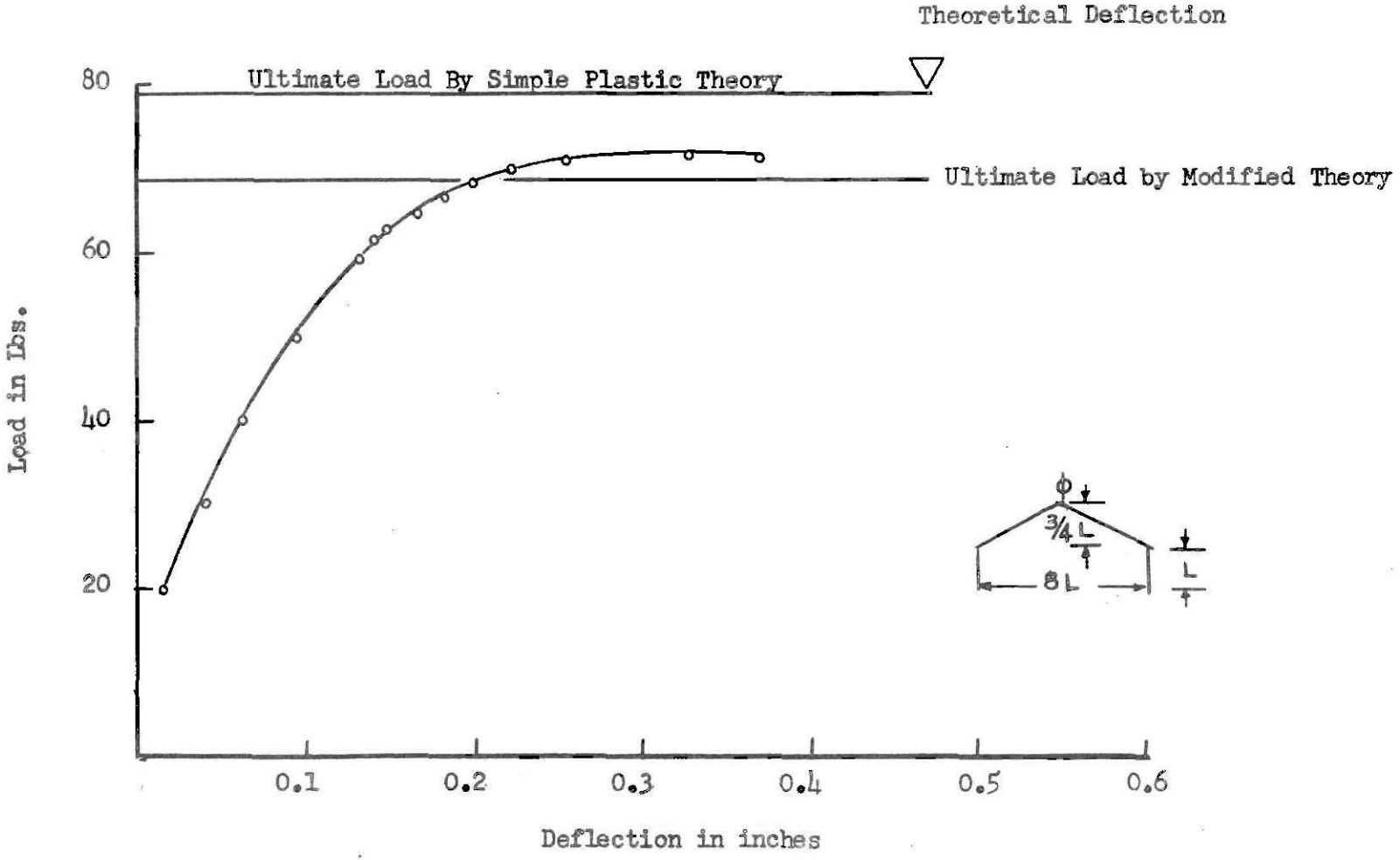

Fig. 42. Vertical Deflection of the Apex for Test II-4

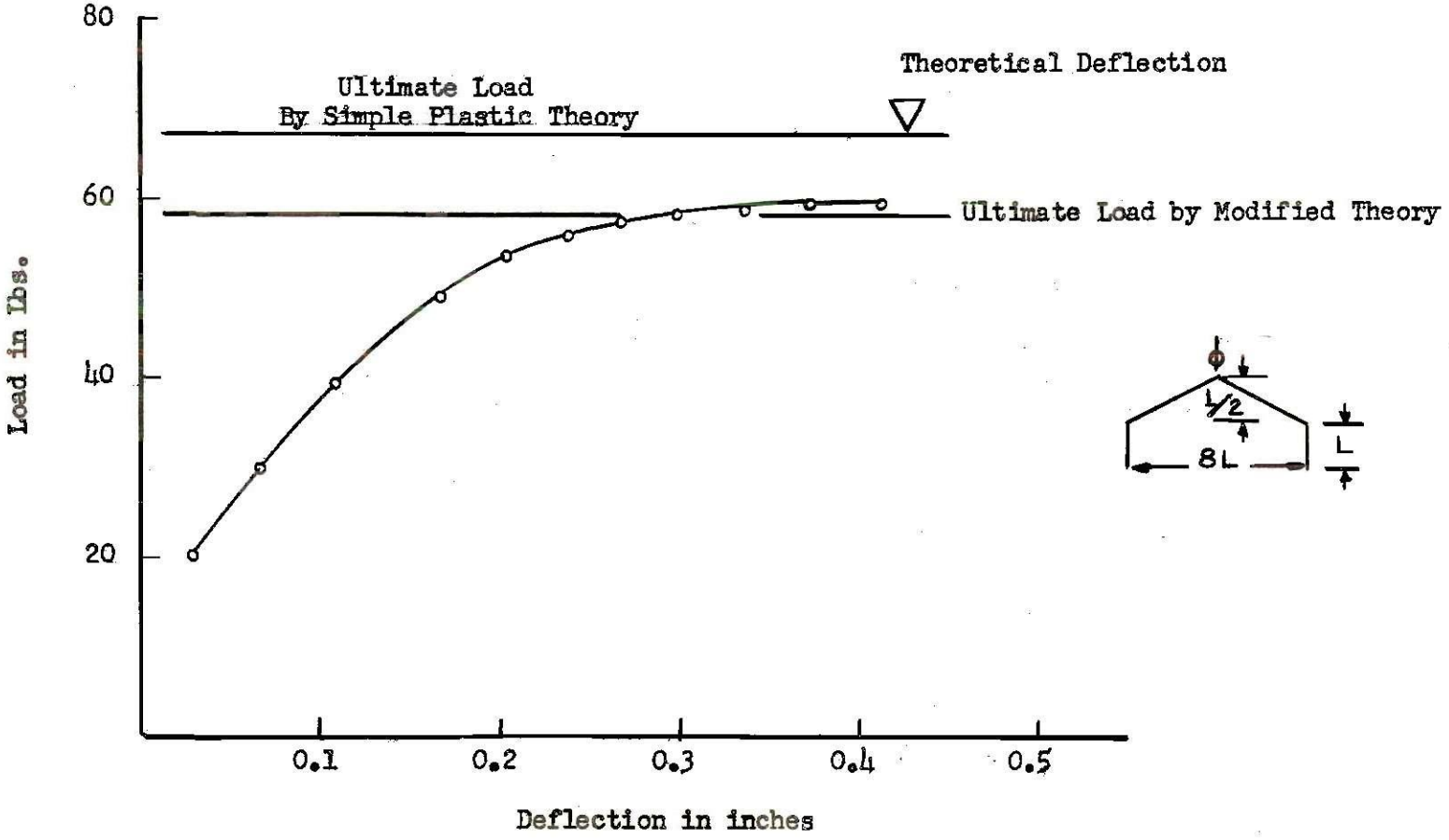

Fig. 43. Vertical Deflection of the Apex for Test II-5

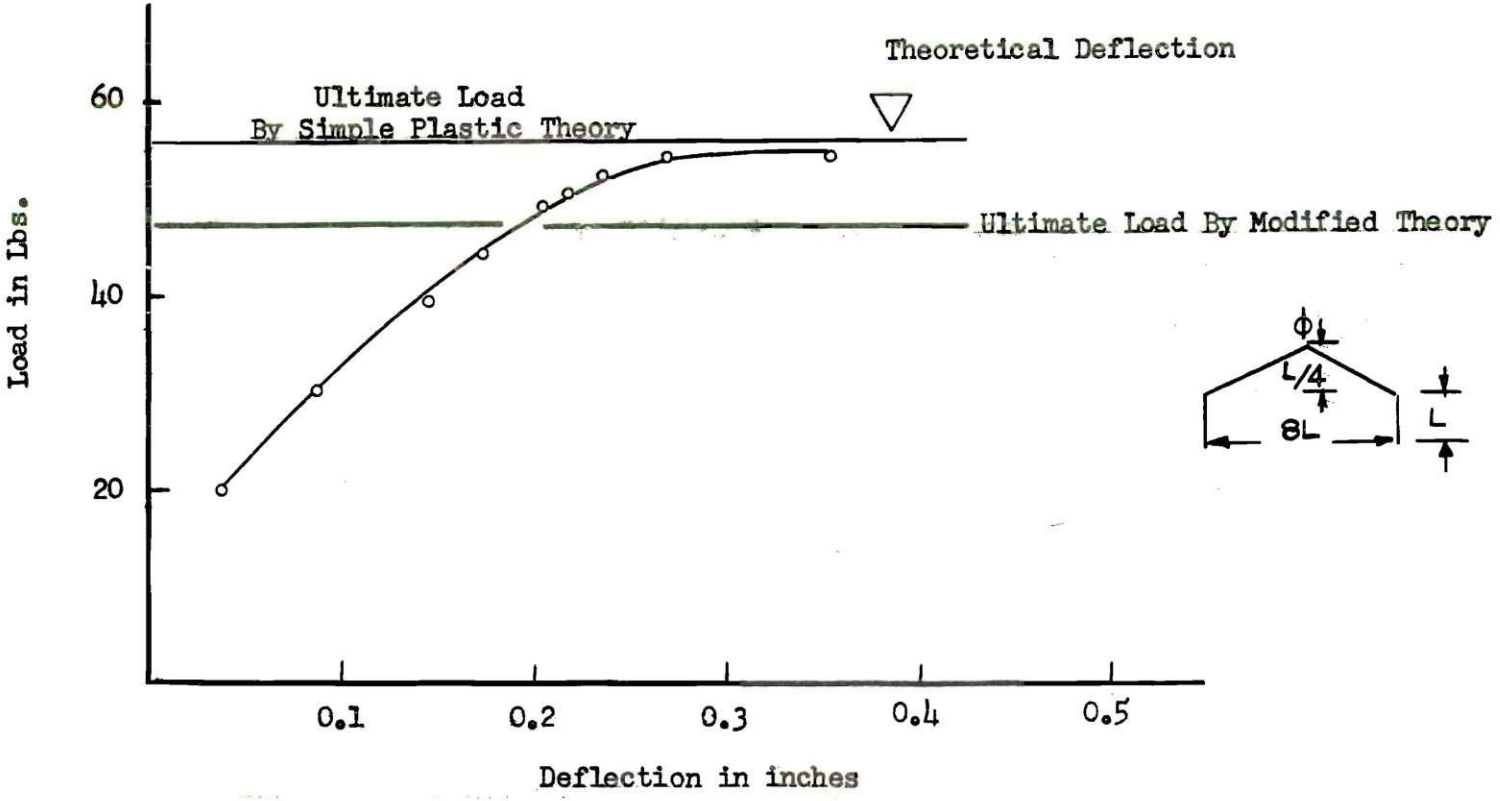

Fig. 44. Vertical Deflection of the Apex for Test II-6

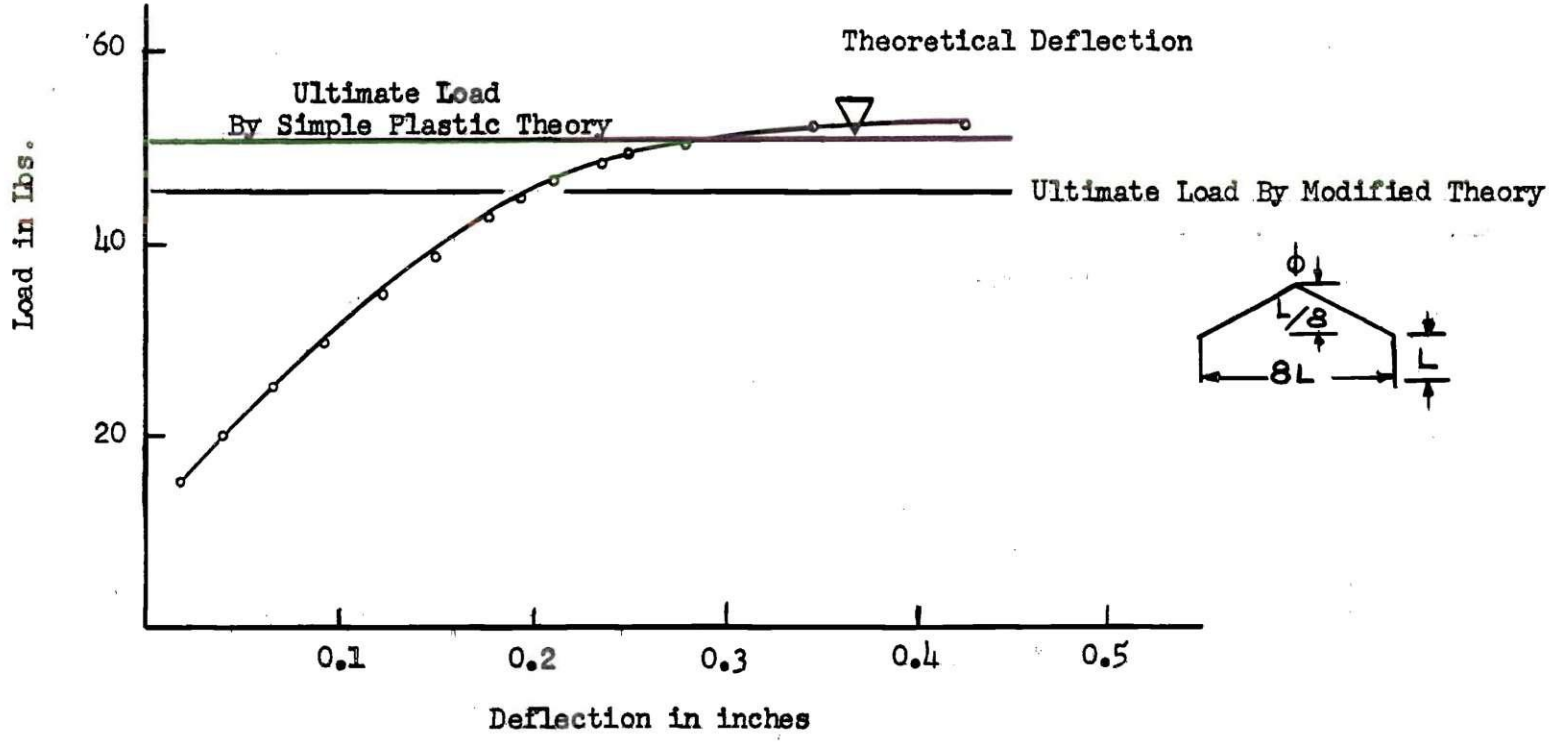

Fig. 45. Vertical Deflection of the Apex for Test II-7

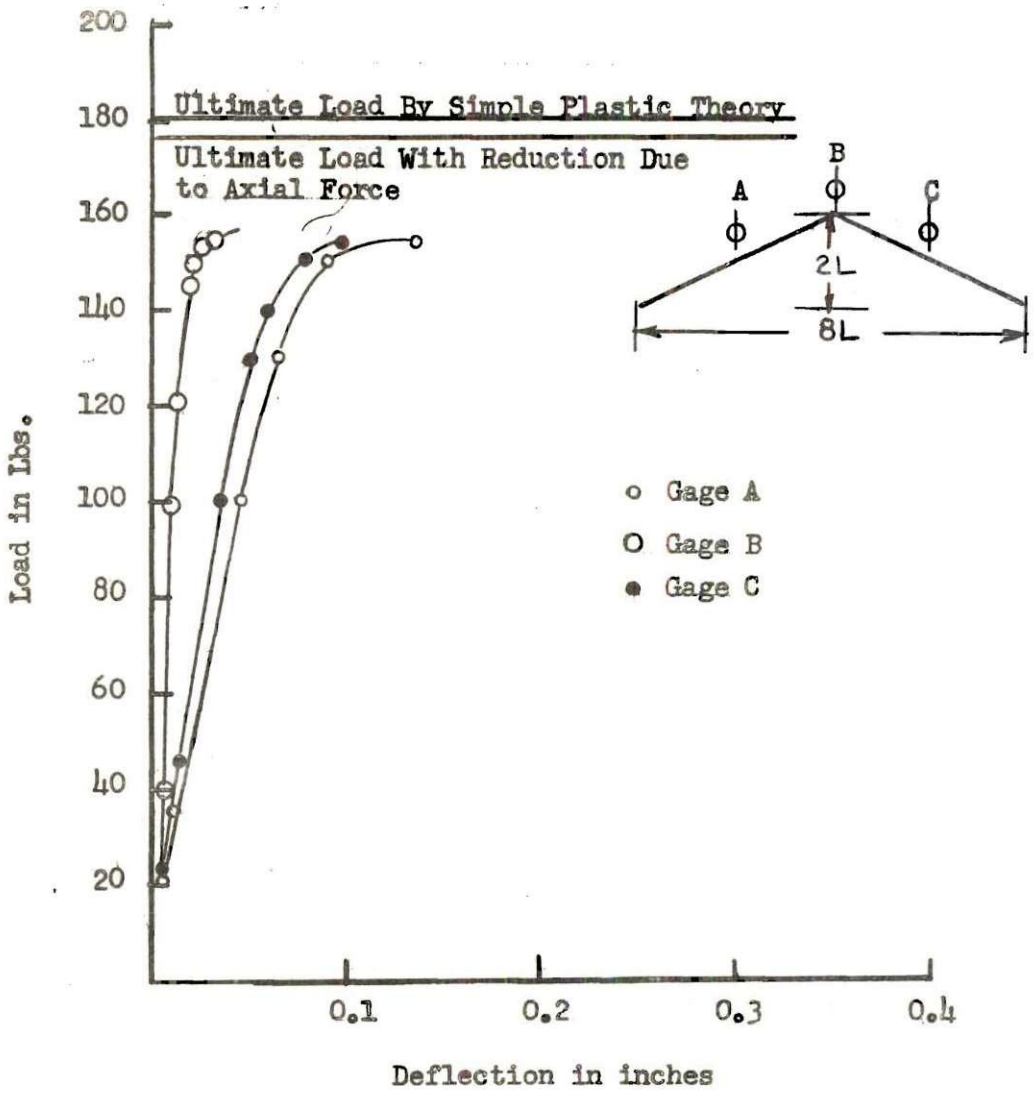

Fig. 46. Vertical Deflections for Test III-1

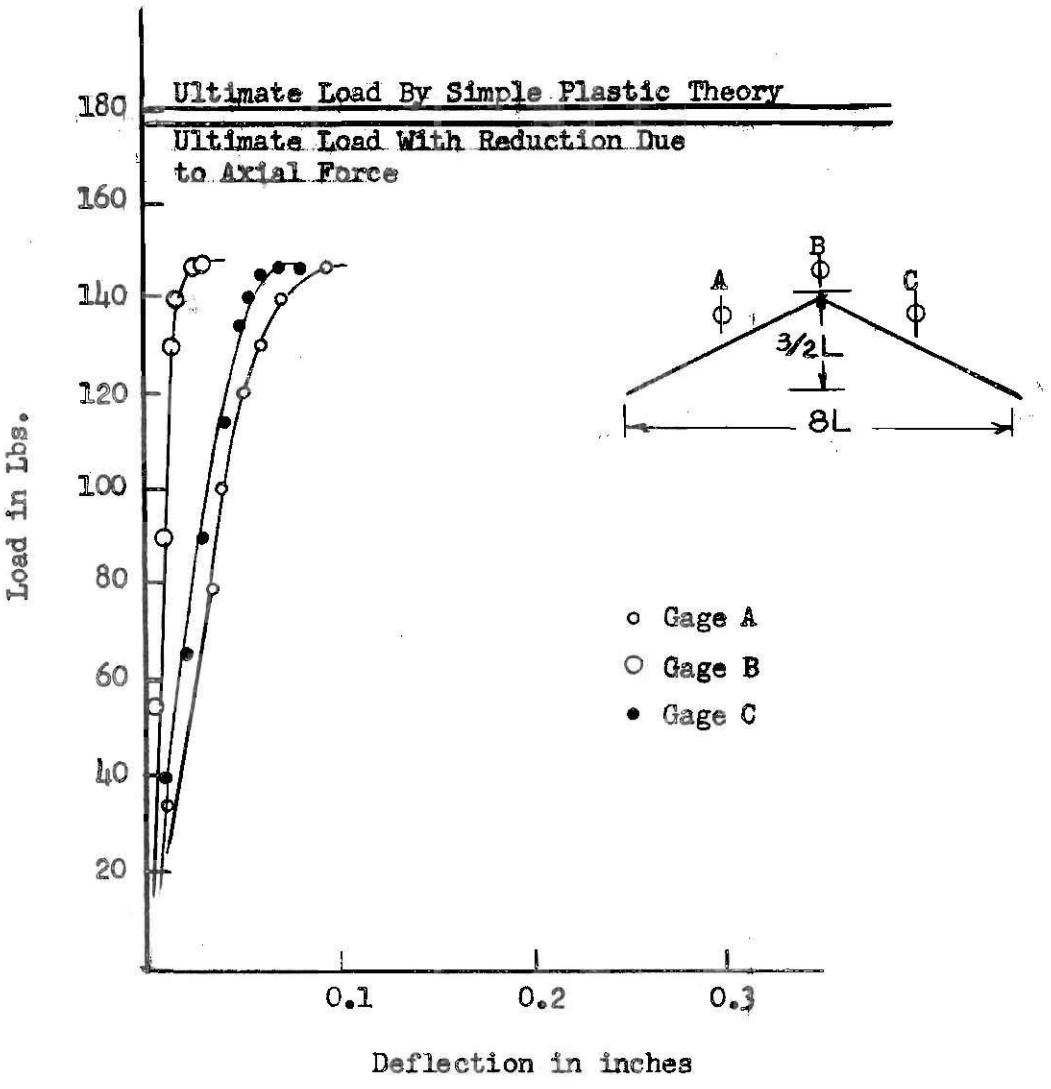

Fig. 47. Vertical Deflections for Test III-2

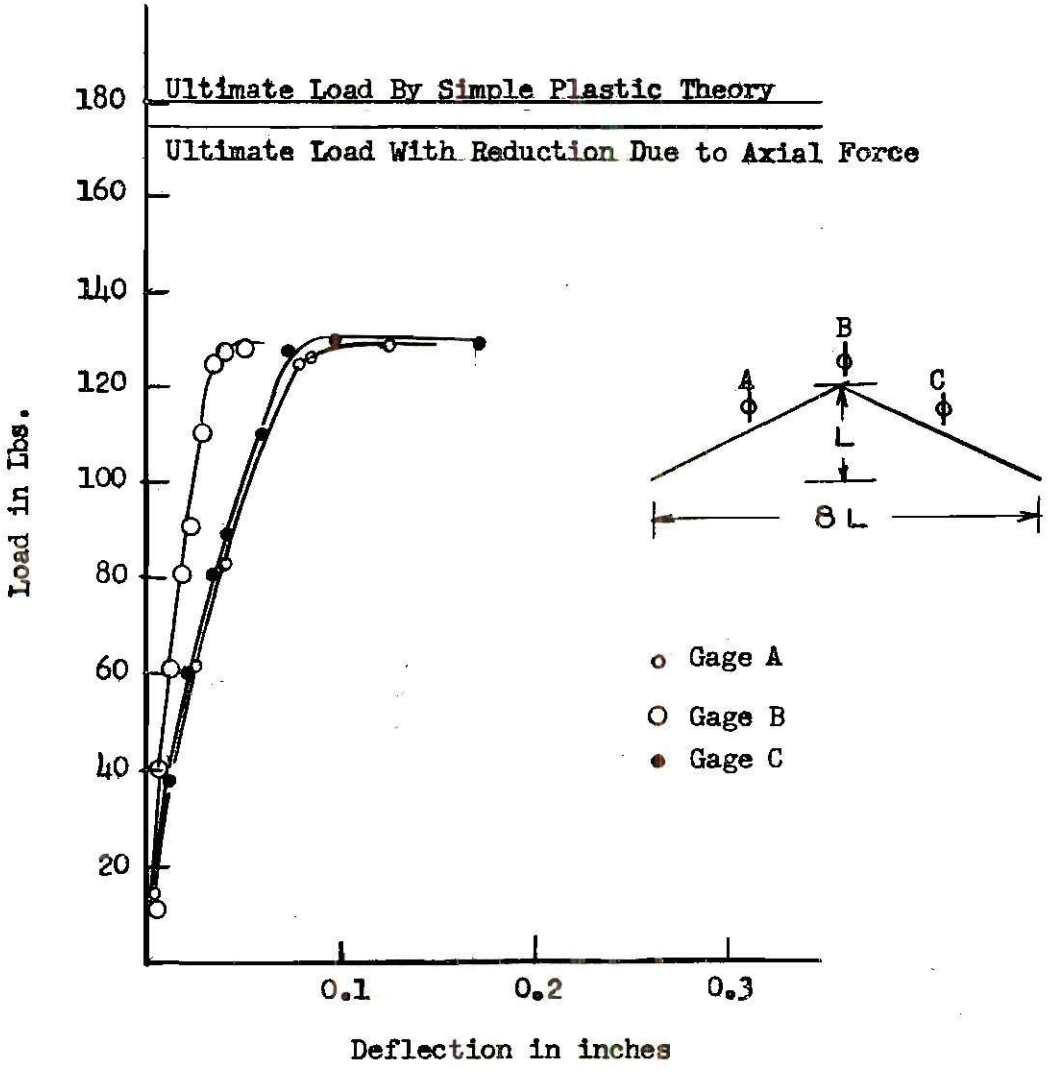

Fig. 48. Vertical Deflections for Test III-3

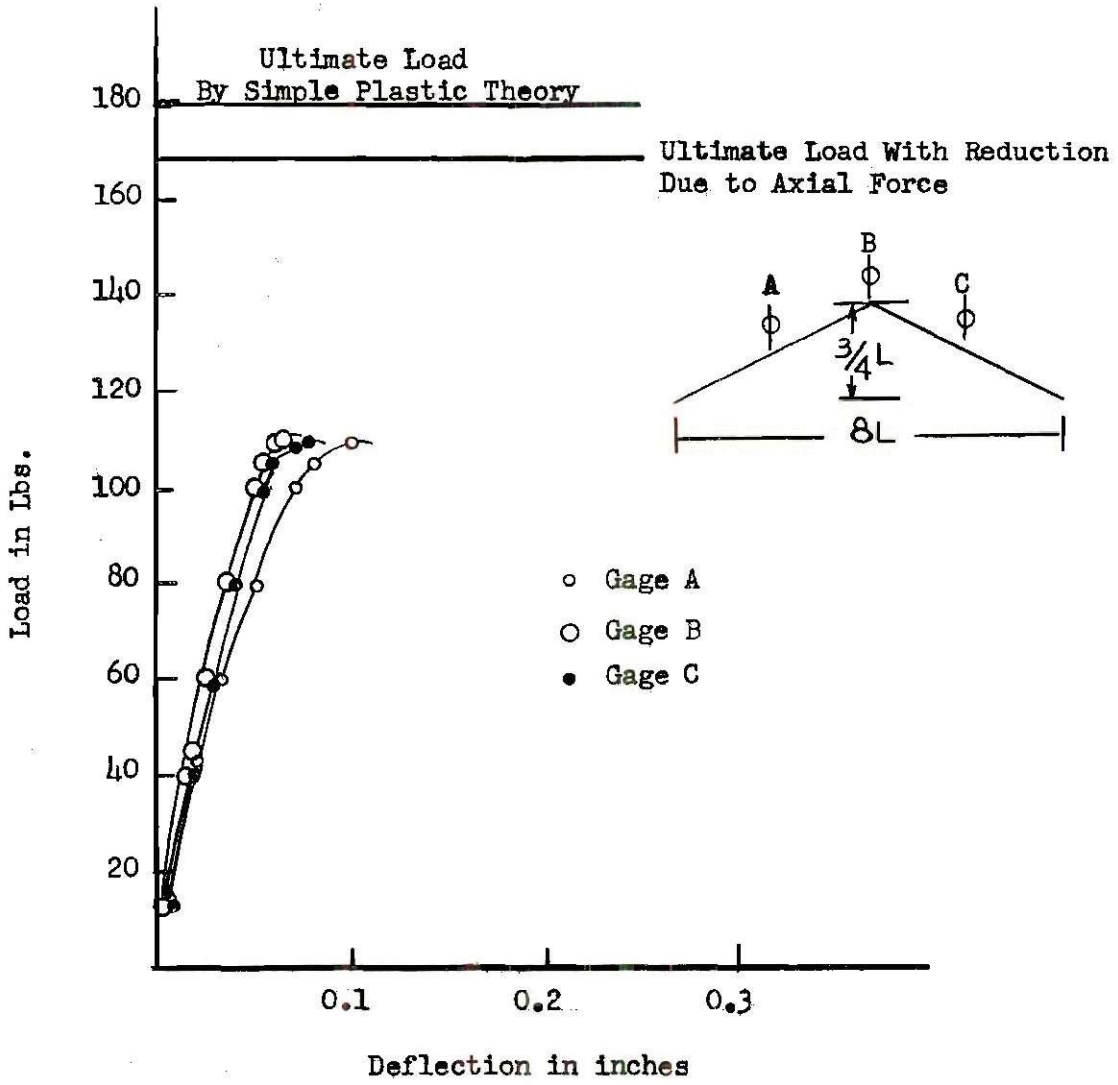

Fig. 49. Vertical Deflections for Test III-4

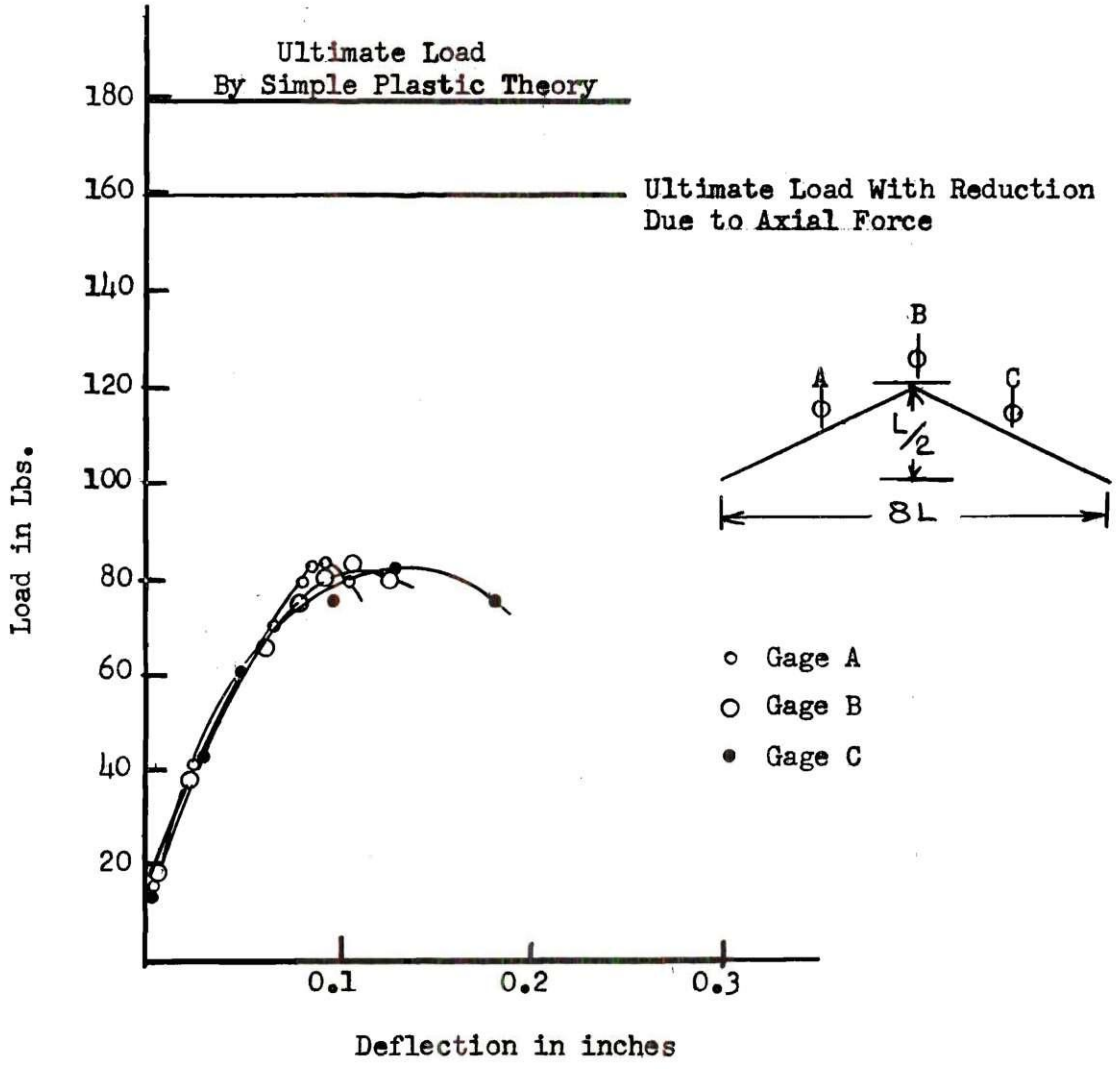

Fig. 50. Vertical Deflections for Test III-5

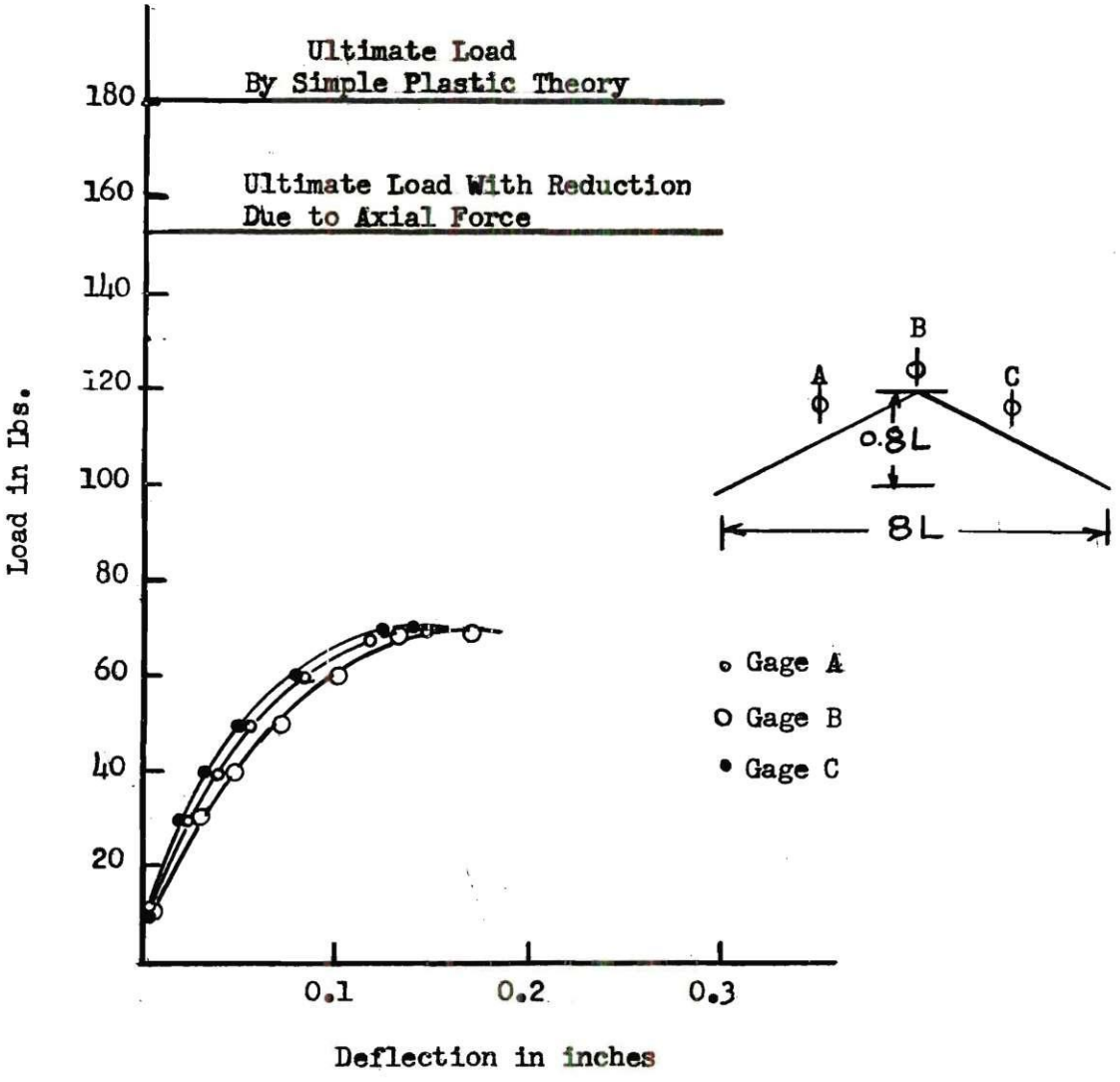

Fig. 51. Vertical Deflections for Test III-6

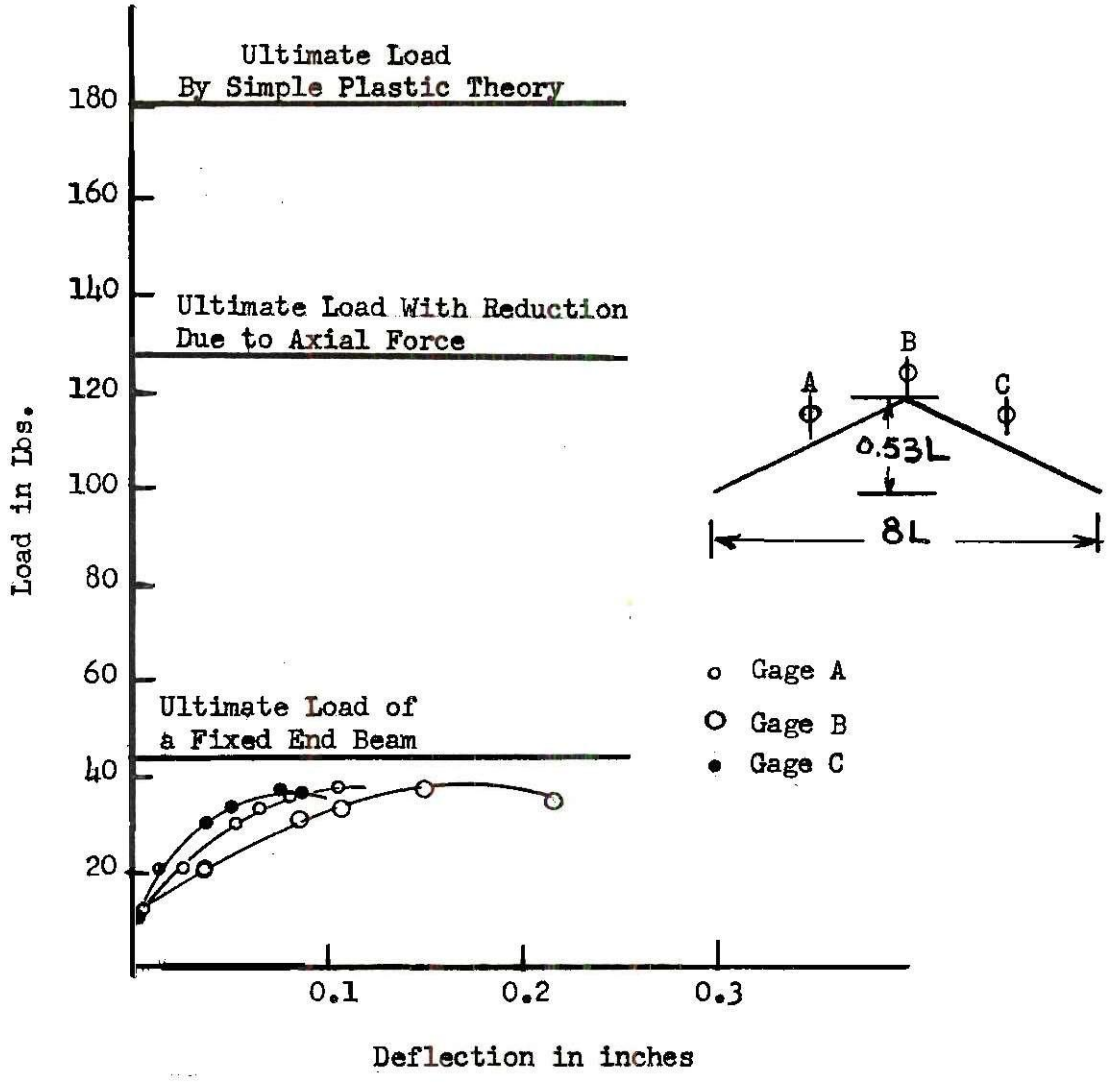

Fig. 52. Vertical Deflections for Test III-7

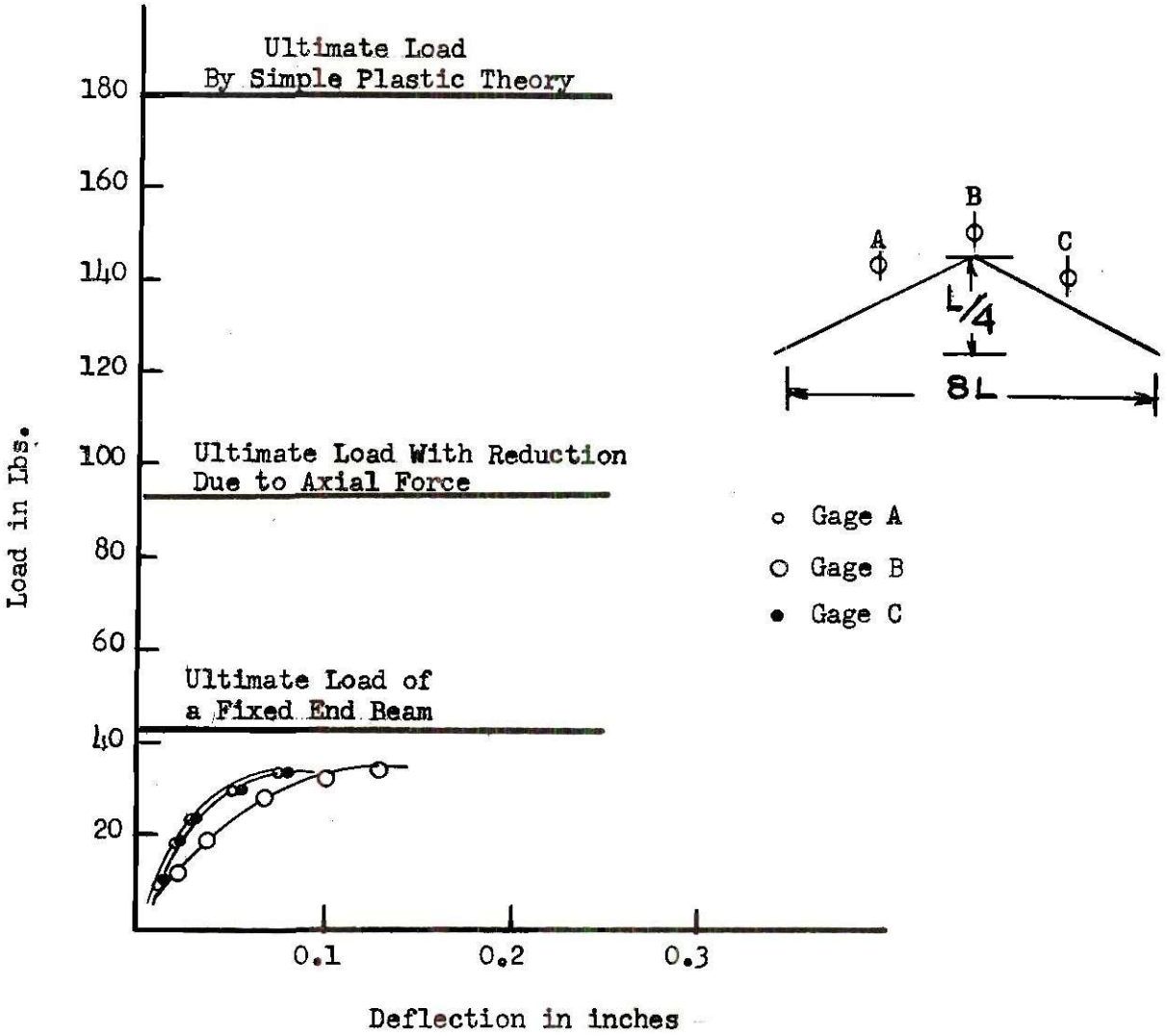

Fig. 53. Vertical Deflections for Test III-8

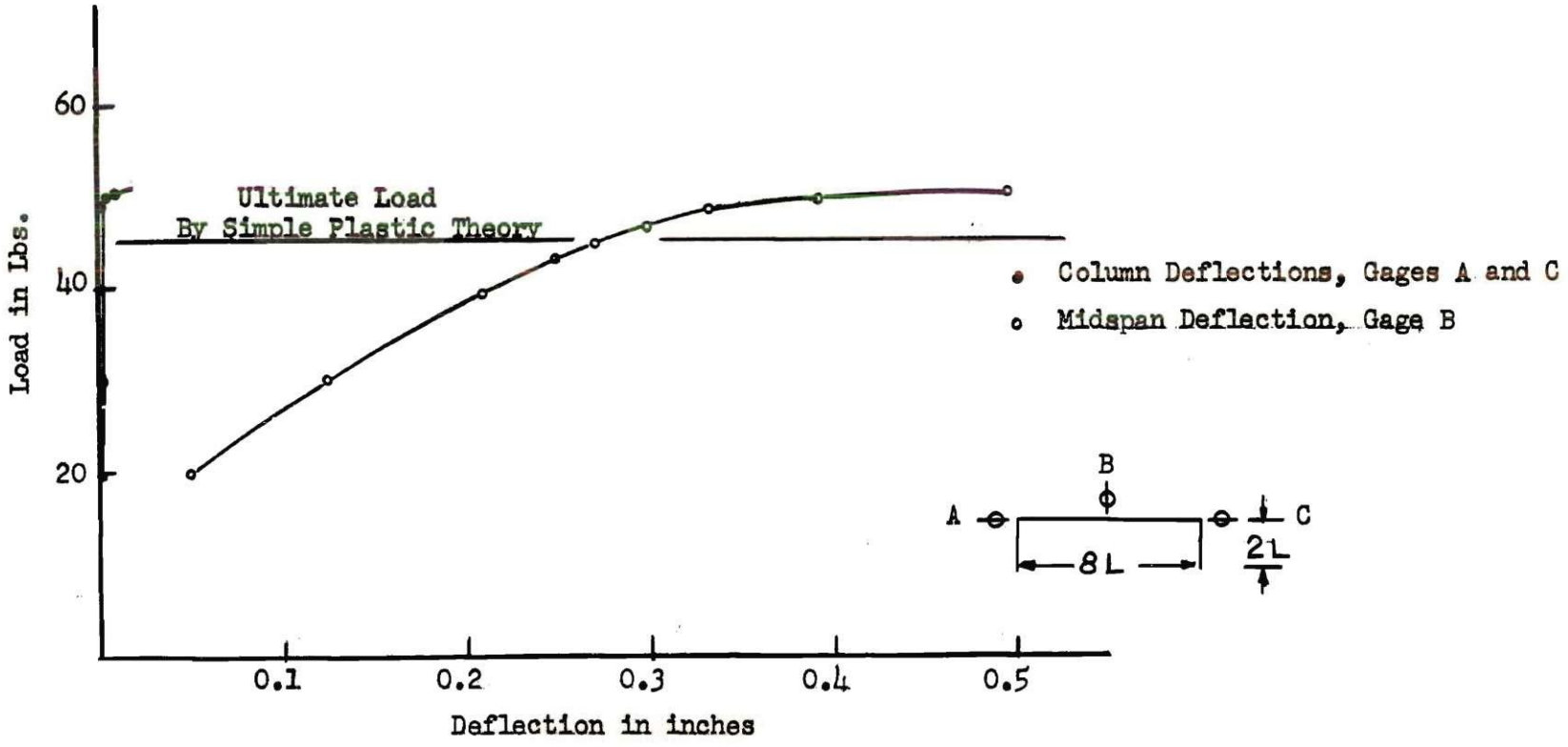

Fig. 54. Horizontal and Vertical Deflections for Test P-1

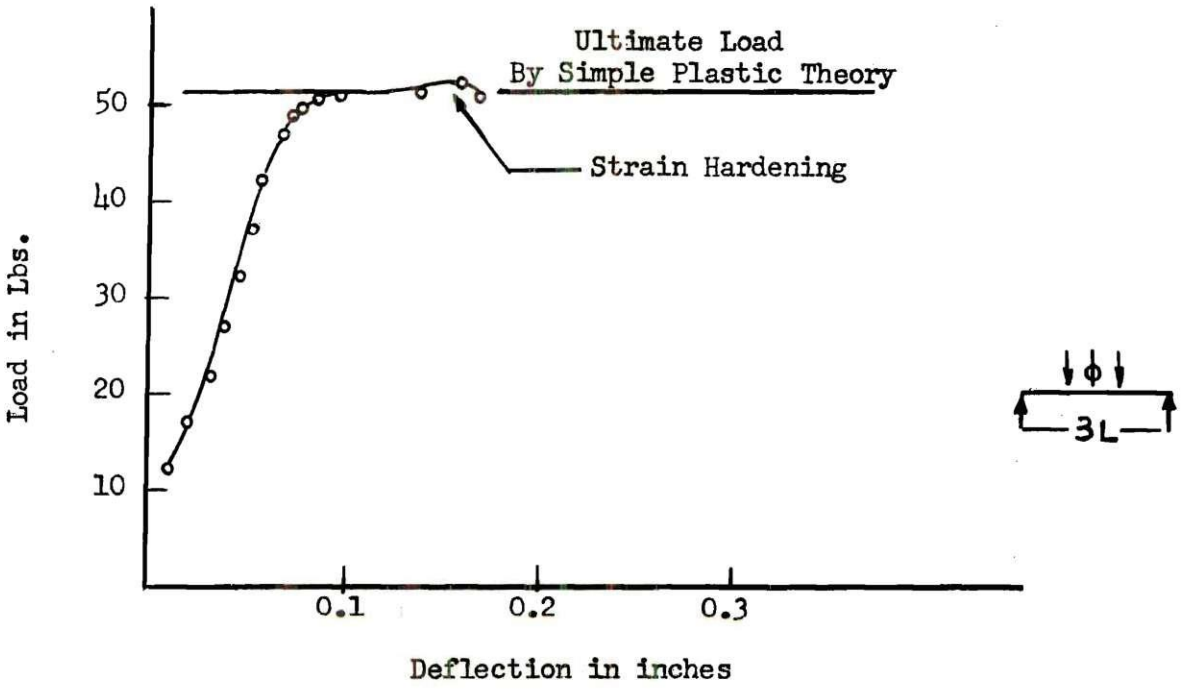

Fig. 55. Midspan Deflection for Test B-1

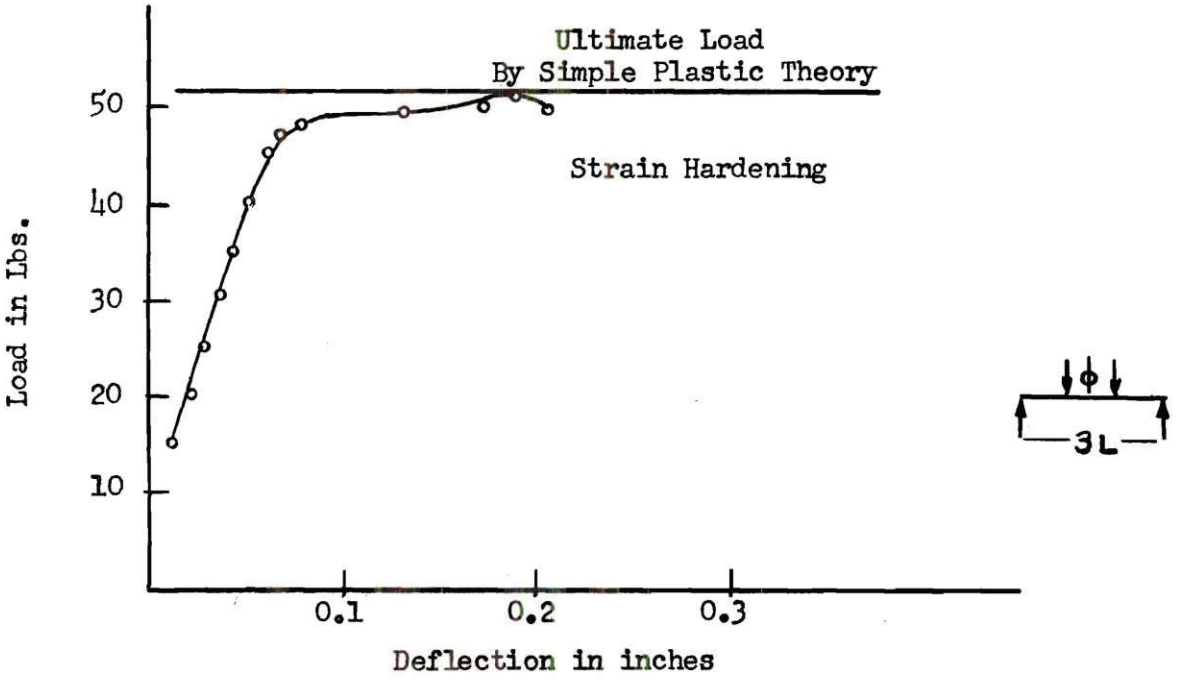

Fig. 56. Midspan Deflection for Test B-2

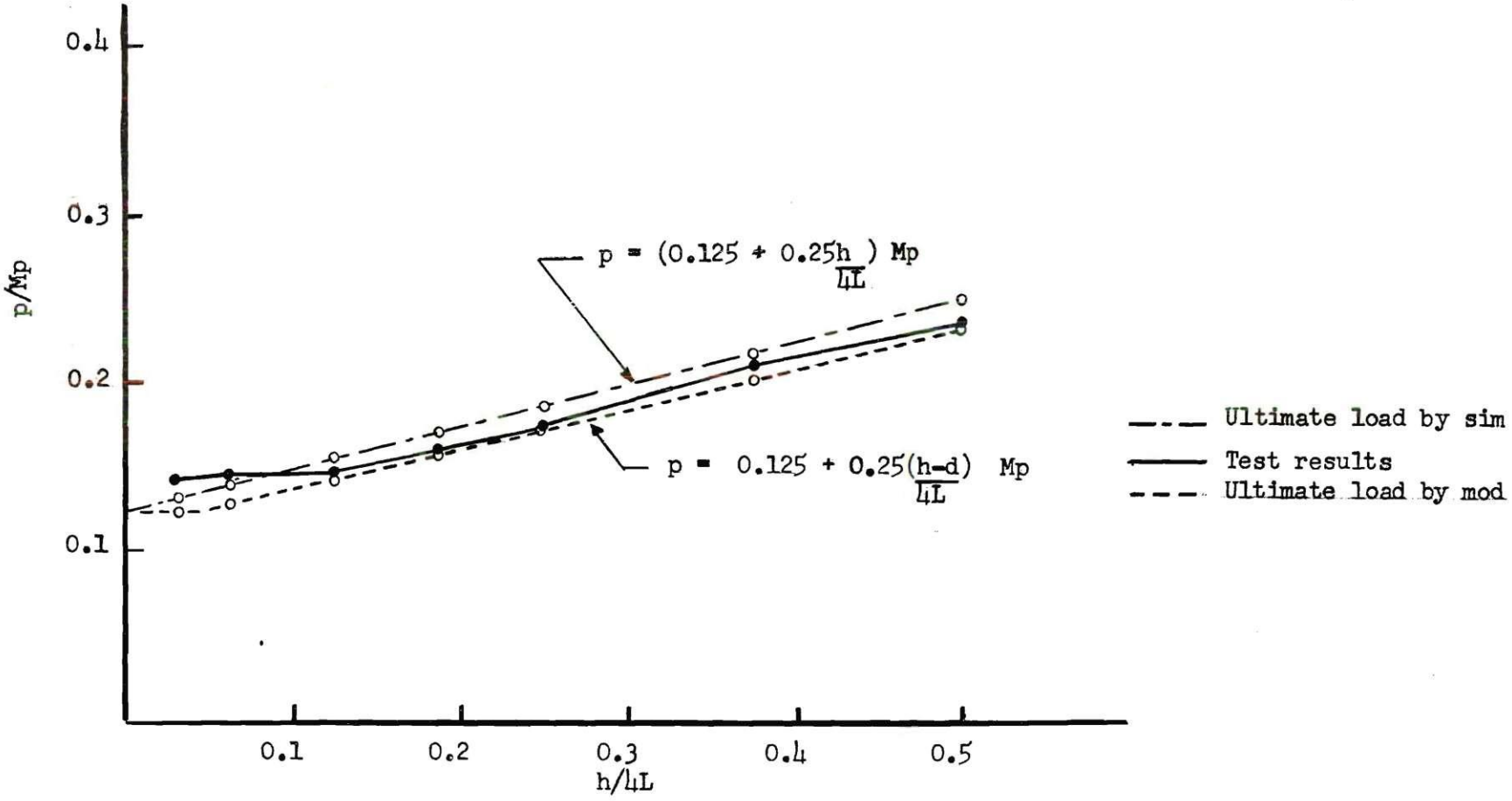

Fig. 57. Summary of Results for Models Type I

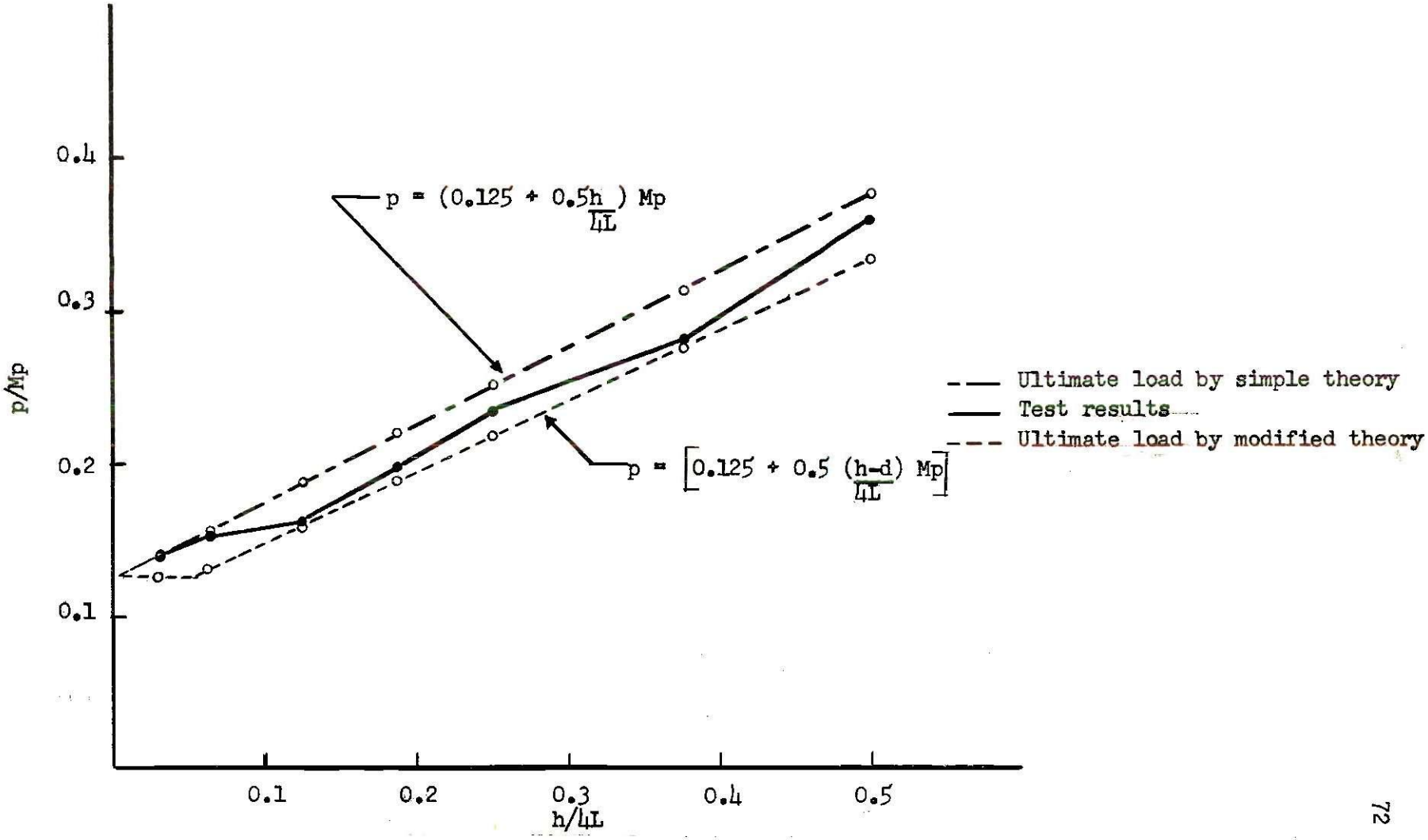

Fig. 58. Summary of Results for Models Type II

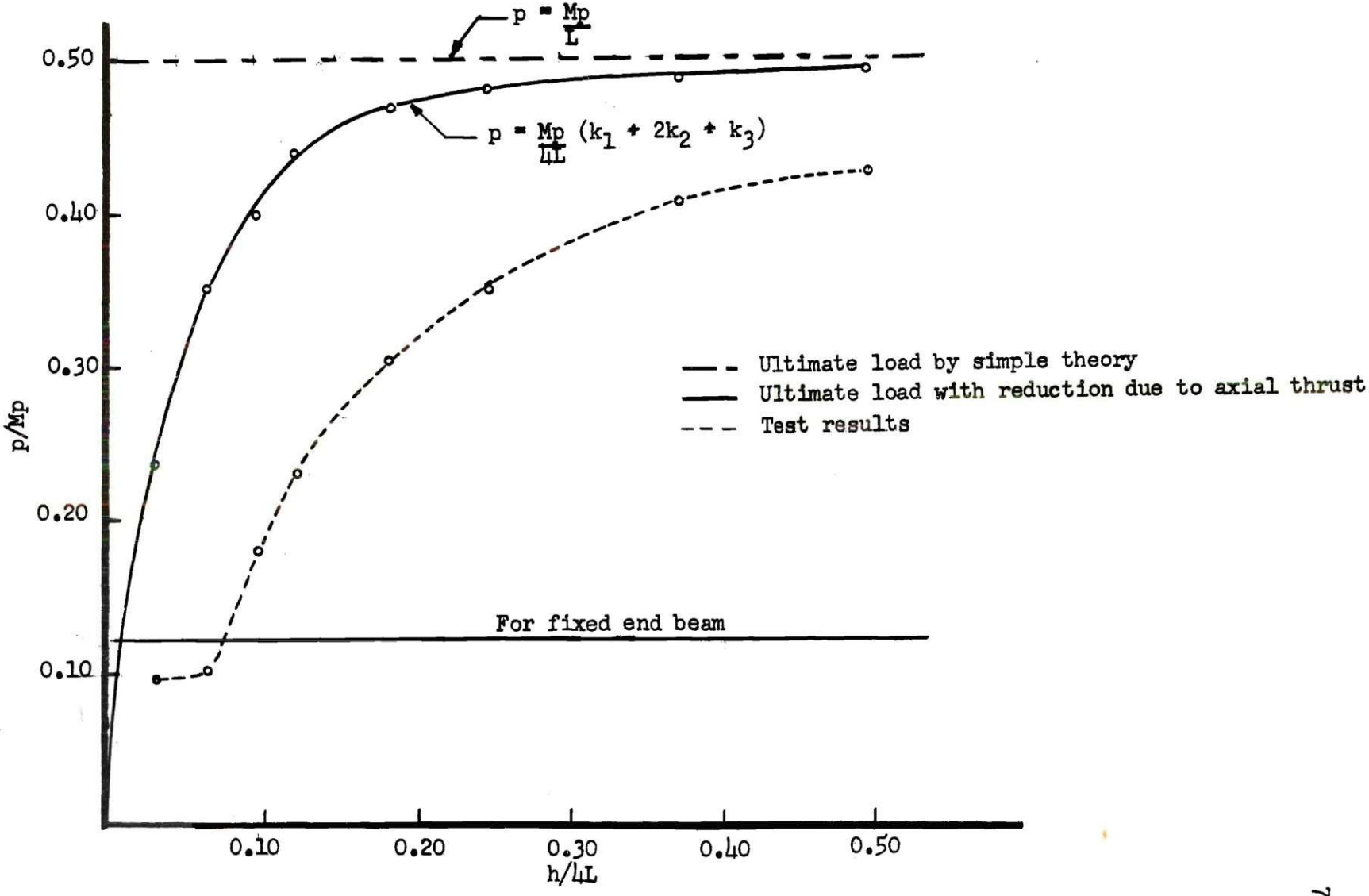

Fig. 59. Summary of Results for Models Type III

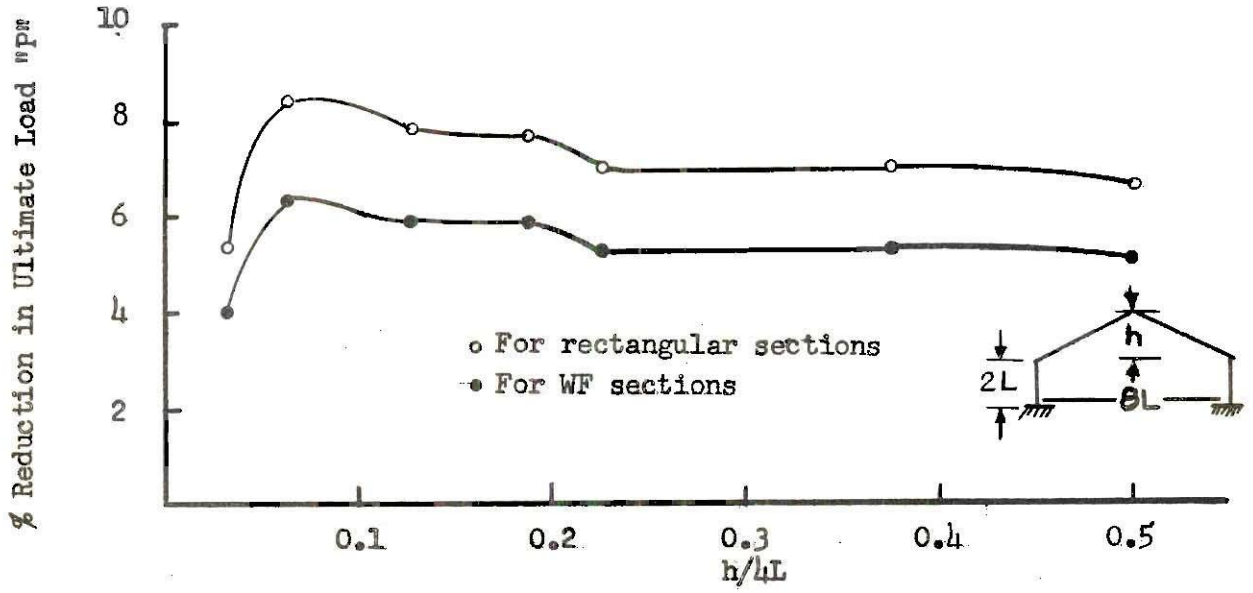

Fig. 60. Effect of Deflection on Ultimate Load for Frames Type I

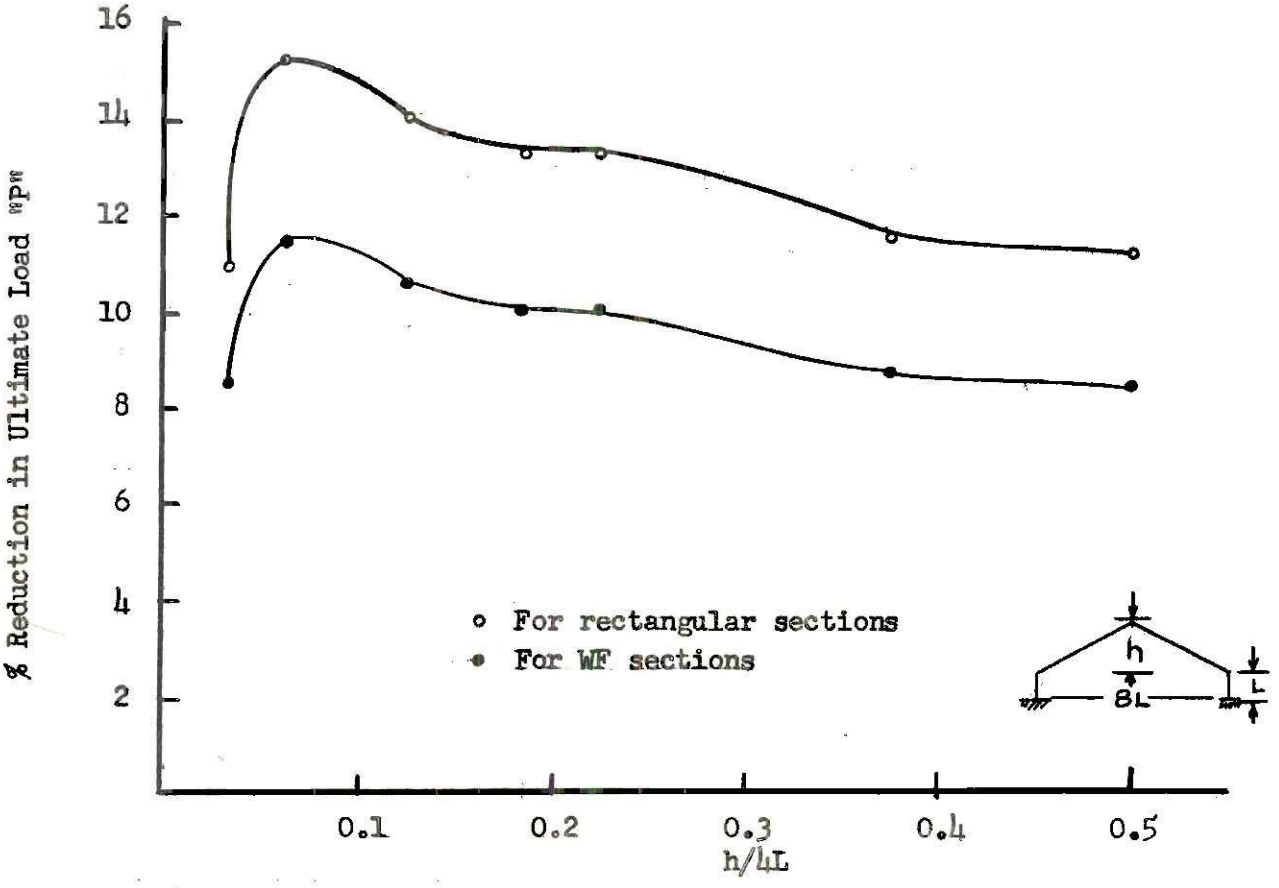

Fig. 61. Effect of Deflection on Ultimate Load for Frames Type II

APPENDIX B

TABLES

Table 1. Model Dimensions

Types	I-1	I-2	I-3	I-4	I-5	I-6	I-7	II-1	II-2	II-3	II-4	II-5	II-6	II-7
h	4.0	3.0	2.0	1.5	1.0	0.5	0.25	4.0	3.0	2.0	1.5	1.0	0.5	0.25
L	2.0	2.0	2.0	2.0	2.0	2.0	2.0	2.0	2.0	2.0	2.0	2.0	2.0	2.0

Types	III-1	III-2	III-3	III-4	III-5	III-6	III-7	III-8	P-1	B-1	B-2
h	4.0	3.0	2.0	1.5	1.0	0.8	0.53	0.25	--	--	--
L	2.0	2.0	2.0	2.0	2.0	2.0	2.0	2.0	2.0	2.0	2.0

Note: All dimensions are in inches. The above dimensions refer to Fig. 29.

Table 2. Results of Coupon Tension Tests

Coupon Number	Py in lbs.	b in in.	Area of section in sq. in.	σ_y in psi	Mp in in.lbs	E $\times 10^{-6}$ psi	I $\times 10^{4}$ in.^{4}
T-1	1100	0.1875	0.0352	31300	51.5	30	1.03
T-2	1100	0.1875	0.0352	31300	51.5	30	1.03

Note: The above coupons were tested with an Olsen "Super L" Hydraulic Universal Testing Machine.

Table 3. Results of Beam Tests

Test	P in lbs.	Mp in in. lbs.	Average Mp in in. lbs.
B-1	52	52	51.5
B-2	51	51	51.5

Table 4. Values of the Constants and of the "k" Factors

Type	A	B	C	D	E	F	G	H	I	k_1	k_2	k_3
I-1	0.01024	0.02048	0.01024	0.01505	0.02043	0.00458	0.01047	0.01047	0.00000	0.998	0.998	0.999
I-2	0.00768	0.01795	0.01024	0.01364	0.01725	0.00360	0.01095	0.01095	0.00000	0.998	0.998	0.999
I-3	0.00512	0.01536	0.01024	0.01260	0.01508	0.00249	0.01136	0.01136	0.00000	0.999	0.999	0.999
I-4	0.00384	0.01409	0.01024	0.01220	0.01408	0.00189	0.01149	0.01149	0.00000	0.999	0.999	0.999
I-5	0.00256	0.01280	0.01024	0.01192	0.01319	0.00127	0.01160	0.01160	0.00000	0.999	0.999	0.999
I-6	0.00128	0.01150	0.01024	0.01176	0.01240	0.00064	0.01168	0.01168	0.00000	0.999	0.999	0.999
I-7	0.00064	0.01089	0.01024	0.01172	0.01203	0.00032	0.01169	0.01169	0.00000	0.999	0.999	0.999
II-1	0.02048	0.03072	0.01024	0.03010	0.03548	0.00458	0.02094	0.02094	0.00000	0.996	0.995	0.998
II-7	0.00128	0.01150	0.01024	0.02342	0.02370	0.00032	0.02338	0.02338	0.00000	0.999	0.997	0.997
III-1	0.01968	0.06134	0.04066	0.01705	0.05508	0.03804	0.01049	0.04198	0.03148	0.985	0.988	0.992
III-2	0.02184	0.07292	0.05108	0.01977	0.06878	0.04902	0.01463	0.05850	0.04387	0.979	0.981	0.986
III-3	0.02772	0.10094	0.07322	0.02630	0.09810	0.07180	0.02275	0.09100	0.06825	0.962	0.964	0.969
III-4	0.03451	0.13047	0.09596	0.03343	0.12830	0.09487	0.03072	0.12290	0.09217	0.938	0.941	0.946
III-5	0.04910	0.19139	0.14228	0.04817	0.18952	0.14134	0.04659	0.18634	0.13975	0.884	0.886	0.890
III-6	0.06020	0.23600	0.17600	0.05900	0.23380	0.17490	0.05810	0.23200	0.17400	0.841	0.843	0.846
III-7	0.09473	0.37636	0.28163	0.09436	0.37563	0.28126	0.09345	0.37380	0.28035	0.711	0.712	0.715
III-8	0.18807	0.75100	0.56291	0.18788	0.75061	0.56273	0.18742	0.74970	0.56227	0.479	0.479	0.481

Table 5. Summary of the Results of Tests on Models Types I and II

Type	Theoretical "P" in Lbs.	Modified "P" in Lbs	Test Results "P" in Lbs.	Reduction[1]	Reduction[2]	Difference[3] in Percent	dv Theoretical in Inches	dv Test in Inches
I-1	90.5	84.5	86.5	6.6	4.4	2.9	0.51	0.43
I-2	79.2	73.5	75.0	7.0	5.3	2.0	0.47	0.39
I-3	67.5	62.8	63.6	7.0	5.8	0.2	0.43	0.38
I-4	62.3	57.5	58.5	7.7	6.0	0.2	0.41	0.34
I-5	56.4	52.0	53.5	7.8	5.2	0.3	0.39	0.32
I-6*	51.0	46.7	53.5	8.4	-	-	0.36	0.44
I-7*	47.5	45.0	52.0	5.3	-	-	0.35	0.43
II-1	135.0	120.0	125.0	11.2	7.4	4.1	0.69	0.50
II-2	112.5	99.6	100.5	11.5	10.6	0.9	0.58	0.44
II-3	90.5	78.5	82.0	13.3	9.4	4.5	0.51	0.40
II-4	79.0	68.5	71.5	13.3	9.5	4.4	0.47	0.33
II-5	67.5	58.0	59.0	14.0	12.6	0.2	0.43	0.37
II-6*	56.3	47.7	55.0	15.2	-	-	0.38	0.43
II-7*	50.5	45.0	52.0	10.9	-	-	0.36	0.43

[1] Reduction due to deflection difference between "P" theoretical and "P" modified in percent.

[2] Reduction due to deflection difference between "P" theoretical and "P" of test in percent.

[3] Difference between "P" Modified and "P" of test in percent.

* The explanation of the results of these tests is given on page 29.

Table 6. Summary of the Results of Tests on Models Type III

Type	Theoretical Load "P" in Lbs.	Test Results Load "P" in Lbs.	Reduction Due to Axial Load in %	Reduction Due to Deflections in %	Total Reduction in %
III-1	180.5	154.5	1.3	13.1	14.4
III-2	180.5	147.0	1.9	16.6	18.5
III-3	180.5	128.0	3.6	25.5	29.1
III-4	180.5	109.0	5.9	33.6	39.5
III-5	180.5	84.0	11.4	42.0	53.4
III-6	180.5	65.0	15.7	48.4	64.1
III-7	180.5	36.6	28.8	50.8	79.6
III-8	180.5	34.8	52.1	28.6	80.7

APPENDIX C

A SEMI-GRAPHICAL DETERMINATION OF THE REDUCTION FACTORS DUE TO AXIAL FORCE FOR WF SECTIONS

A SEMI-GRAPHICAL DETERMINATION OF THE REDUCTION FACTORS DUE AXIAL FORCE FOR WF SECTIONS

The method of finding the "k" values for any frame having WF members can be simplified by using a semi-graphical approach. This method is adequate for design purposes. An example to illustrate this is shown below:

Assume a 18WF50 is to be used in a frame similar to Type I-1 with L = 5'-0" (see Fig. 62):

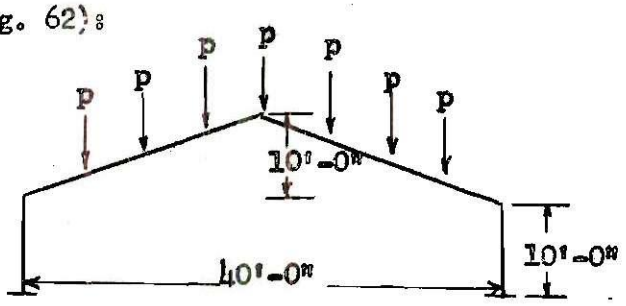

Fig. 62

From Eq. (10):

$$p = \frac{Mp}{8L}(k_1 + 2k_2 + k_3)$$

From Eqs. (15), (16), and (17) we have:

$$A_1 = \frac{7p}{2}$$

$$A_2 = H\cos\alpha + R\sin\alpha$$

$$A_3 = H\cos\alpha$$

A_1 from Eq. (18) will be:

$$A_1 = \frac{7Mp}{16L}(k_1 + 2k_2 + k_3)$$

From Eq. (4) we have:

$$Py = Ay = \frac{Mp}{Z} A$$

then:

$$\frac{A_1}{Ay} = \frac{7Z}{16L(A)}(k_1 + 2k_2 + k_3) \qquad (99)$$

For A_2, using Eqs. (22) and (4) we get:

$$A_2 = \frac{Mp}{2L}(k_1 + k_2)\frac{4L}{\sqrt{20L^2}} + \frac{7Mp}{16L}(k_1 + 2k_2 + k_3)\frac{2L}{\sqrt{20L^2}} \qquad (100)$$

$$\frac{A_2}{Ay} = \frac{2Z}{A\sqrt{20L^2}}(k_1 + k_2) + \frac{7Z}{8A\sqrt{20L^2}}(k_1 + 2k_2 + k_3) \qquad (101)$$

For A_3, using Eqs. (28) and (4) we obtain:

$$A_3 = \frac{Mp}{2L}(k_1 + k_2)\frac{4L}{\sqrt{20L^2}} \qquad (102)$$

$$\frac{A_3}{Ay} = \frac{2Z}{A\sqrt{20L^2}}(k_1 + k_2) \qquad (103)$$

For an 18WF50 from AISC(3):

$A = 14.71$ sq. in.

$Z = 1.14 \times 89 = 101.46$ in.^{3}

Substituting the values of L, A, and Z in Eqs. (84), (85), and (86):

$$\frac{A_1}{Ay} = 0.0504k_1 + 0.1080k_2 + 0.0504k_3 \tag{104}$$

$$\frac{A_2}{Ay} = 0.0738k_1 + 0.0962k_2 + 0.0224k_3 \tag{105}$$

$$\frac{A_3}{Ay} = 0.0514k_1 + 0.0514k_2 \tag{106}$$

Assuming all "k's" to be equal, we have:

$$\frac{A_1}{Ay} = 0.2160k \tag{107}$$

$$\frac{A_2}{Ay} = 0.1924k \tag{108}$$

$$\frac{A_3}{Ay} = 0.1028k \tag{109}$$

Now these equations can be written in the form shown below:

$$\frac{A_1}{Ay} = Ck_1 \tag{110}$$

$$\frac{A_2}{Ay} = Ck_2 \tag{111}$$

$$\frac{A_2}{Ay} = Ck_3 \tag{112}$$

Since $\frac{A_1}{Ay}$ is greater than $\frac{A_2}{Ay}$, we use $\frac{A_1}{Ay}$ in the determination of k_2.
The values of C for k_1, k_2, and k_3 are as follows:

For k_1: C = 0.2160

For k_2: $C = 0.2160$

For k_3: $C = 0.1028$

From Fig. 63 we obtain:

$k_1 = 0.95$ $k_2 = 0.95$ $k_3 = 0.98$

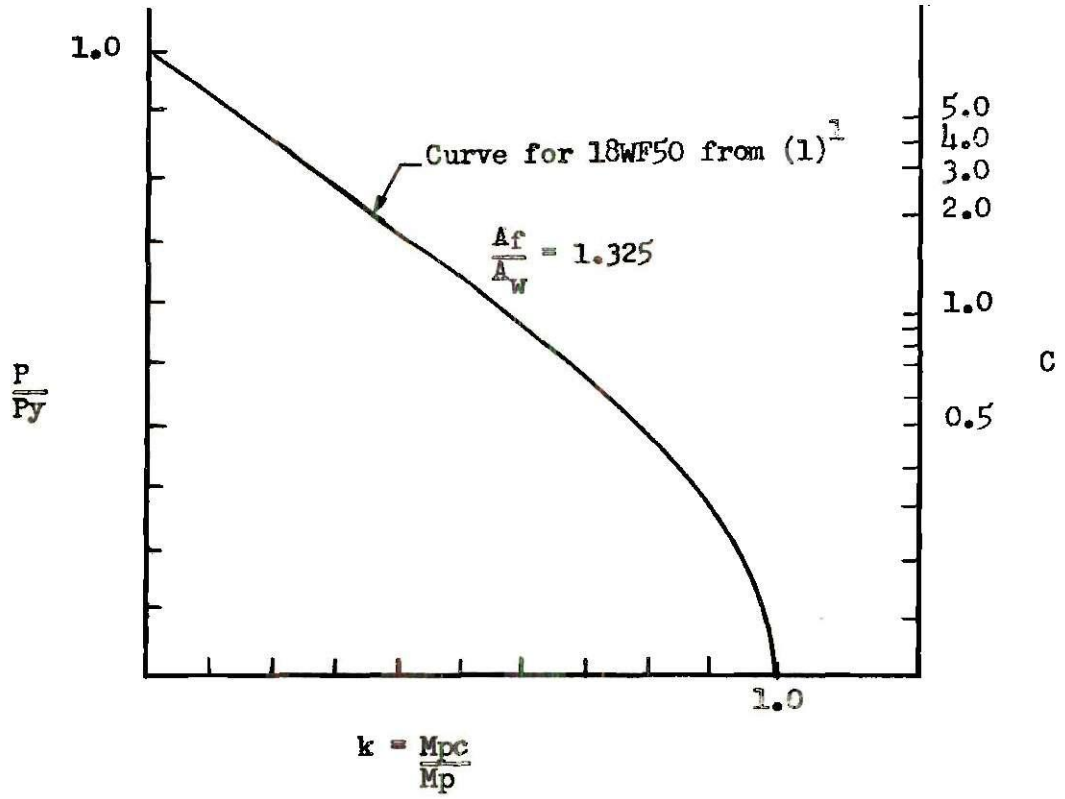

Fig. 63. Axial Load and Moment Interaction Curve for an 18WF50

---

[1] For neutral axis in the web:

$$\frac{Mpc}{Mp} = 1 - \frac{A^2}{4wZ}\left(\frac{P}{Py}\right)^2$$

For neutral axis in the flange:

$$\frac{Mpc}{Mp} = \frac{A^2}{bZ}\left[t - \left(1 - \frac{P}{Py}\right)\right]\left[d - t + \left(1 - \frac{P}{Py}\right)\right]$$

To find the values of "k_1", "k_2", and "k_3", we enter the chart in Fig. 63 on the right with the value of "C" as determined from the previous calculations. We then go horizontally to the left until we intersect the interaction curve and go down vertically to intersect the "$\frac{Mpc}{Mp}$" axis, which in turn gives us the desired value of "k".

To obtain more accurate values of "k", substitute the values obtained from this first trial in Eqs. (110), (111), and (112) and repeat the procedure.

An analysis was conducted for a frame similar to Type II-1 with L = 5'-0" using 18WF50 sections. The values of "C" and "k" were as follows:

For k_1: C = 0.3168

For k_2: C = 0.3400

For k_3: C = 0.2056

From Fig. 63 we obtain:

$k_1 = 0.89$ $k_2 = 0.87$ $k_3 = 0.95$

BIBLIOGRAPHY

LITERATURE CITED

(1) Beedle, Lynn S., Bruno Thurlimann, and Robert L. Ketter, Plastic Design in Structural Steel, Lecture Notes, Lehigh University and American Institute of Steel Construction, Bethlehem, Pennsylvania, Sept. 1955.

(2) Neal, B. G., The Plastic Methods of Structural Analysis, Wiley & Sons, Inc., New York, New York, 1956.

(3) Steel Construction Manual, Fifth edition, New York, New York; American Institute of Steel Construction, 1955.